

OC415-1 Cruise Report

Draft – July 22, 2005

Contents:

1. Objectives
2. Selection of the candidate features
3. Transects through the candidate features
4. Selection of the target feature
5. Detailed sampling of the target cyclone C1
6. Temporal evolution of the target cyclone C1
5. Detailed sampling of the target feature A4
6. Additional sampling in cyclone C5
7. Why is the biological response so different in cyclones and anticyclones?
8. Cruise narrative
- Appendix 1. Selected maps and calibration plots
- Appendix 2. VPR Deployments
- Appendix 3. MOCNESS tows
- Appendix 4: Incubations
- Appendix 5: URI underway sampling calibrations (Horne)
- Appendix 6: Cruise participants

1. Objectives

Voyage 415-1 of R/V *Oceanus* was the first cruise of the 2005 field season of the Eddy Dynamics, Mixing, Export, and Species composition (EDDIES) project. A detailed description of the EDDIES science plan is contained in the original proposal, available on the project web site¹. The specific objectives of this cruise “Survey 1” were to:

1. Select several candidate eddy features on the basis of satellite altimetry and ocean color.
2. Obtain precise determinations of eddy centers for each of the candidate eddy features (XBT, ADCP).
3. Occupy transects through the center of each of the candidate features (XBT, CTD/Rosette, MOCNESS, VPR, Light probe)
4. Choose target feature based on the results of (3)
5. Conduct detailed grid survey of target feature
6. Repeat (5) as time allows to assess temporal evolution of the target feature
7. Repeat (3) as time allows to assess temporal evolution of other features
8. Coordinate with R/V *Weatherbird II* in joint sampling operations (last 10 days)

2. Selection of the candidate features

¹ http://science.whoi.edu/users/mcgillic/eddies/EDDIES_Project.html

Prior experience suggests that there are at least three different types of mid-ocean eddies in the Sargasso Sea (Figure 1): cyclones, anticyclones, and mode-water eddies (MWEs). Cyclones and MWEs are of interest to this project, as both tend to displace upper ocean isopycnals toward the surface, causing nutrient input into the euphotic zone. Whereas cyclones are identifiable in satellite altimetry by virtue of their negative sea level anomaly (SLA), MWEs are not distinguishable from anticyclones on the basis of altimetry alone because both result in positive SLA. In principle, satellite-based SST could distinguish these two, as anticyclone and MWEs would be characterized by warm and cold SST anomalies, respectively. However, given the paucity of reliable SST imagery in the Sargasso Sea during summer, we had to rely on in situ measurements to unequivocally distinguish MWEs from anticyclones.

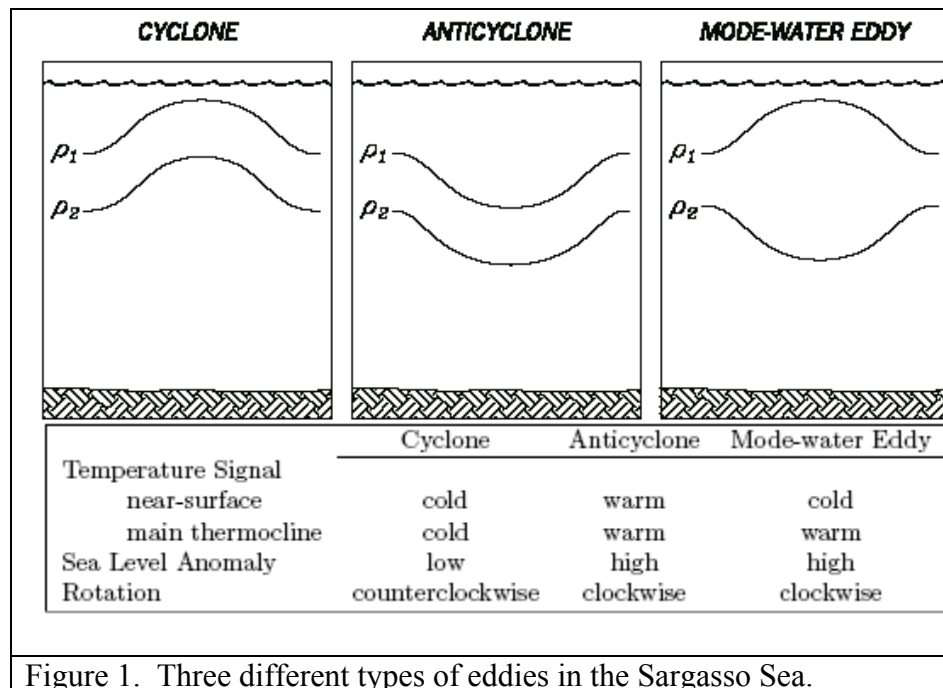


Figure 1. Three different types of eddies in the Sargasso Sea.

Eddy age is another key issue. Whereas an intensifying cyclone will have upwelling in its center, the isopycnals in the interior of a decaying cyclone will be downwelling. The earlier phase of the eddy's lifetime will be when nutrient injection and the associated biological response occur.

Summary of desirable characteristics for the target eddies:

1. Young
2. Strong imprint on upper ocean physics, biology, and chemistry
(not necessarily a large amplitude SLA in the case of a MWE).
3. Intensifying
4. Chemical impact discernible in real time
5. Biological impact discernible in real time
6. Cyclone versus MWE?
 - a. unequivocal satellite determination favors cyclones
 - b. trapping of near-inertial motions and possible enhanced mixing favors MWEs

- c. some of the big events at BATS have been MWEs
 - Jenkins (1988) Summer 1986 event
 - McNeil et al. (1999) July 1995 eddy
- 7. Proximity to BBSR: must be within 1 day's steam for *Weatherbird II*

Clearly, it was necessary to sample several eddies during the first survey cruise prior to making a decision on which feature to target with more detailed sampling.

Eddy statistics from prior years (not shown; see Figure 2 of OC404-1 Cruise Report) provided some guidance with respect to expected eddy trajectories over the course of the planned sampling activities (June-August). With respect to the logistics of the joint operations with the *Weatherbird II*, the ideal eddy would be slightly east of BATS in the beginning (ca. 62W), and slightly west of BATS at the end (ca. 66W).

Eddy features of interest were identified prior to the cruise using satellite altimetry from CCAR² and the Navy³. MODIS ocean color imagery was also made available courtesy of David Siegel and Toby Westberry (UCSB). Five candidate features were selected (Figure 2): two anticyclones (A4,A5) and three cyclones (C3,C4,C5).

All five features were tracked in the satellite data archive to determine their trajectories and recent history of SLA extrema (Figure 3). Cyclone C3 was ESE of BATS in February; its SLA was weak (10-15cm) until apparent intensification in early June (no direct overflight). Cyclone C4 was ESE of BATS in March, and underwent a fairly steady increase in SLA amplitude to nearly -15cm by the end of May. Cyclone C5 was ENE of Bermuda in February, with a persistent SLA of -20-25 cm (note the apparent decay phase in June is a result of altimetric undersampling). Anticyclone A4 was East of BATS in February, exhibiting a fairly persistent SLA of ca. 20cm. Anticyclone A5 can be traced back ENE of Bermuda in March, with a SLA reaching nearly 30cm.

² http://www-ccar.colorado.edu/~realtime/nwatlantic-real-time_ssh

³ <http://www7300.nrlssc.navy.mil/altimetry/>

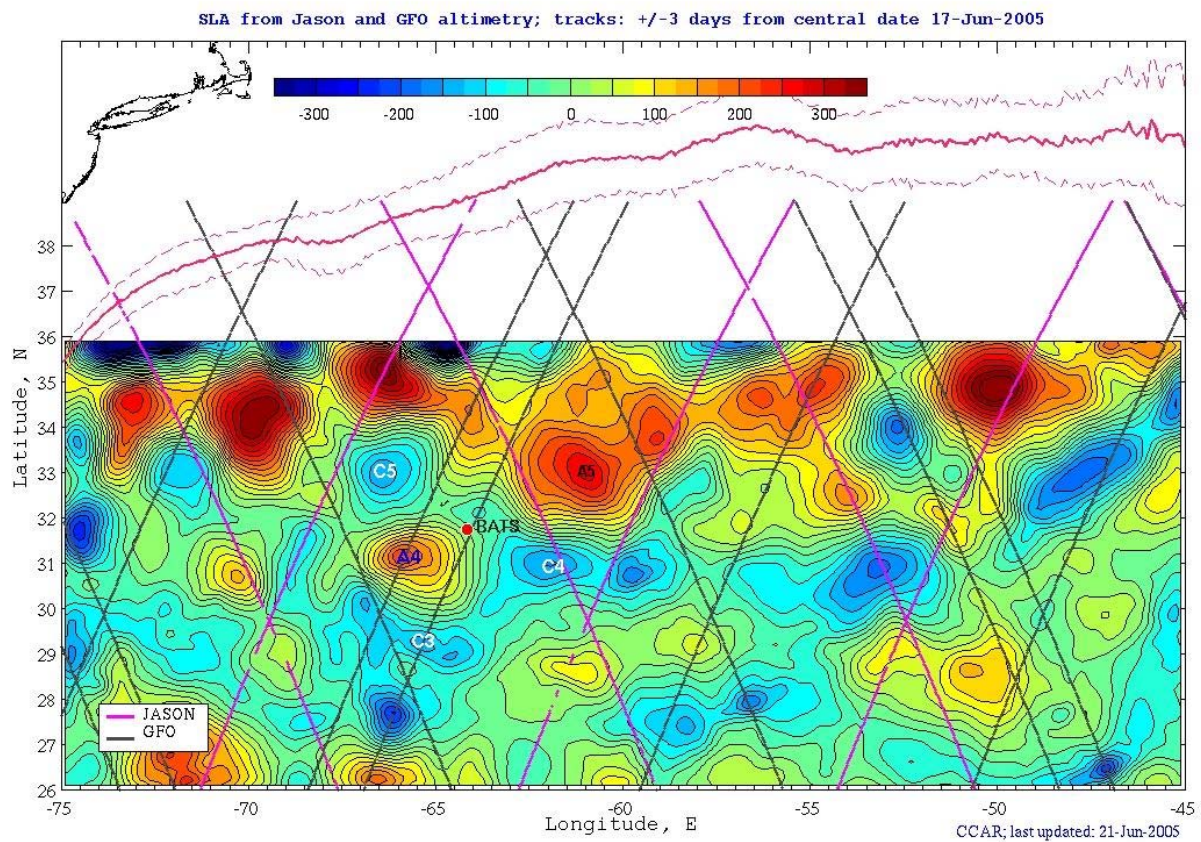
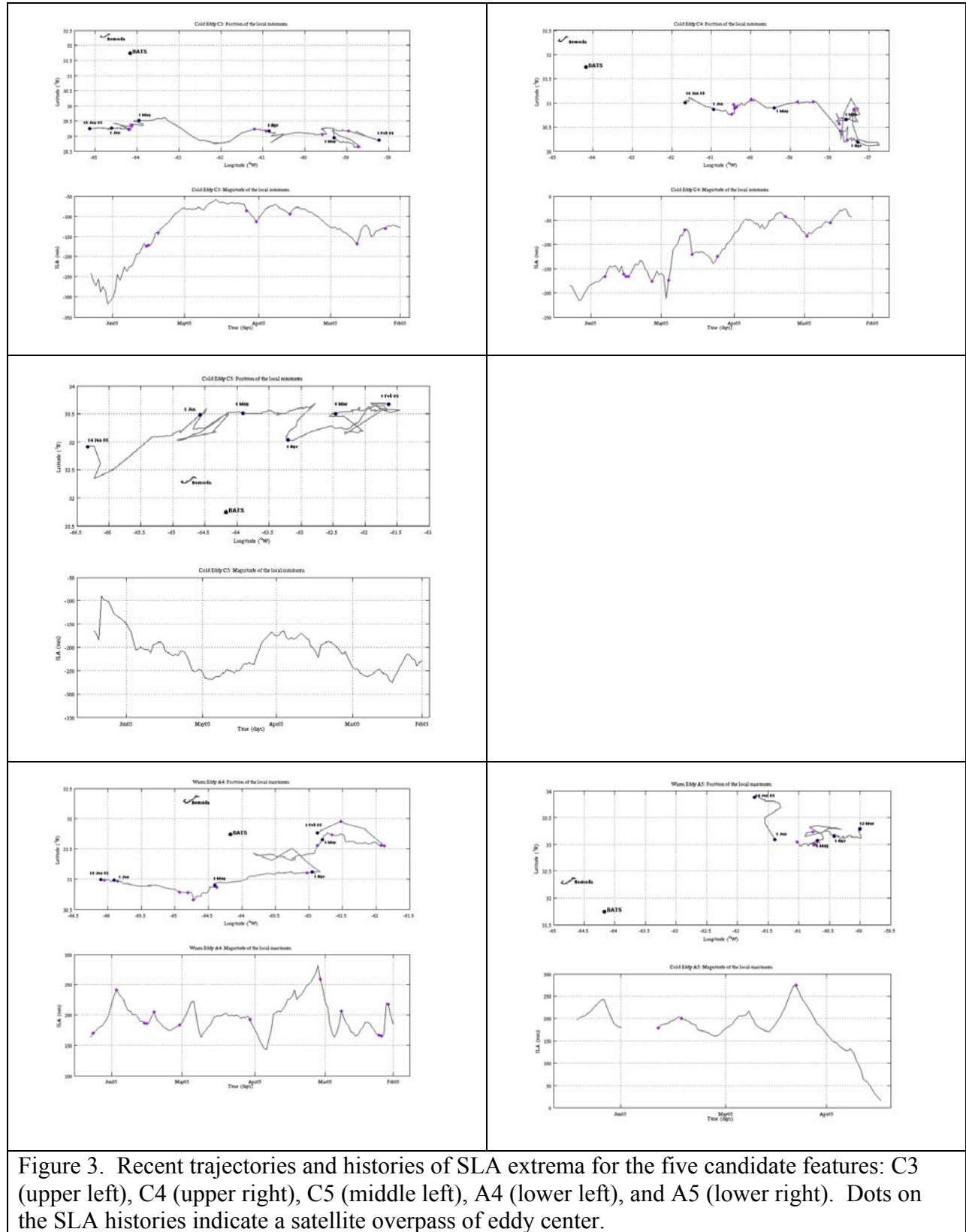


Figure 2. Objective analysis of sea level anomaly (mm) for June 17, 2005. Data source: see footnote (3). Five candidate features are indicated: C3, C4, C5, A4 and A5. The solid magenta line indicates the mean path of the Gulf Stream, and the dashed lines the one standard deviation meander envelope.



4. Selection of the target feature

Cyclone C5 was sampled June 22-23, A4 June 24-26, C3 June 27-28, A5 June 30- July 1. Detailed descriptions of the transects occupied in each of these features follows in the narrative below. Candidate cyclone C4 was not sampled because its SLA expression appeared to degrade during the initial survey phase.

All four eddies have appealing characteristics and would make fine subjects for more detailed study (Table 1; see July 2 narrative). Our choice of the target eddy was based on the evidence we had in hand for the various aspects of the physical-biological-biogeochemical dynamic of interest: an eddy-induced nutrient supply leading to a physiological response in the phytoplankton, a change in species composition, and a change in export flux and biogeochemical cycling. Our observations pertain to the first three aspects; export flux will not be measured until the joint operation with R/V *Weatherbird II* begins.

Nutrient enhancement was evident in all four eddies, as was a physiological response in the phytoplankton community. Changes in phytoplankton species composition and community structure were most evident in anticyclones A4 and A5. However, the prospect that A5 is a relatively rare type of eddy with a distant origin leads to some concern over the degree to which we would be able to generalize the results from a detailed study of that feature. Moreover, the apparent trapping of near-inertial motions and higher vertical shears observed in A4 makes it a compelling candidate for study of mixing processes in the tracer release component of the project led by Jim Ledwell. Therefore A4 was chosen as the target feature.

5. Detailed sampling of the target feature A4

Intensive sampling of A4 began on July 3 with a 3x3 grid of CTD stations spaced 20km apart in the eddy's central core (Figure 0705.1; also see Appendix Figure A1). Temperature maps indicate vertical structure characteristic of a mode-water eddy, with warm anomalies at depth (e.g. 600m) and cold anomalies near surface (e.g. 50m). Maps of fluorescence on level surfaces (upper right) show little organized structure, owing to high-frequency vertical displacements of the subsurface chlorophyll maximum (lower right) associated with internal wave activity (lower left). Averaging the fluorescence data in the 80-120m depth interval yields a more coherent map of the field (Figure 0705.2). The band of highest average fluorescence generally runs SW to NE, but its full extent is not yet delimited by the 3x3 inner grid.

The larger-scale structure of the eddy was mapped in a series of transects occupied July 4-9 (Figures 0709.1-5; also see Appendix Figure A2). High fluorescence at eddy center detected on every transect: (1) SE to NW, (2) N to S, (3) SW to NE, and (4) E to W. Peak fluorescence and doming of the seasonal thermocline are tightly confined to EC. The maximum in fluorescence appeared to decrease over time, although the subsequent VPR survey (July 11-14; see Figure 0714.1) indicates this was a result of a shift in EC during the survey.

Nitrate concentration at EC appears stable over time, remaining enhanced over stations slightly off center (Figures 0709.6; data from Qian Li).

6. Additional sampling in cyclone C5

Given the amplitude of the nutrient enhancement first measured in C5 (Figure 0626.3; data from Qian Li), we were very curious to measure the extent of the ensuing eddy-induced bloom. On July 10-11, we temporarily broke off from our joint operations with the WBII to occupy an additional transect through C5.

Eddy center had moved more than 100km in 17 days since the last occupation, implying a propagation speed of slightly more than 6 km/day. Water mass analysis supports the assertion that this is the same feature we sampled earlier (Figure 0710.1, lower right). Intensity of the feature appears to have diminished, insofar as the magnitude of main thermocline isotherm displacements has lessened from since the last occupation. Data from Qian Li indicates nutrients are still elevated above background levels, but not as much as in the prior occupation.

The VPR transect indicates very low fluorescence overall, with slight enhancement at C5 periphery and in the eddy core (Figure 0710.2). The CTD section of C5 (Figure 0711.1) is consistent with those findings.

7. Why is the biological response so different in cyclones and anticyclones?

The EDDIES observations, together with McNeil et al. (1999) and Sweeney et al. (1999), indicate that diatom blooms occur in mode-water eddies (MWEs) but not in cyclones. Both types of features displace the seasonal pycnocline upward. However, MWEs are also potentially subject to enhanced mixing due to near-inertial wave trapping in anticyclones (Kunze, 1985). Indeed, ADCP measurements indicate enhanced shear in the core of A4 (Figure 0630.2). This enhanced mixing could influence the stoichiometry of limiting nutrients at the base of the euphotic zone. An enigmatic aspect of the background profile on which both operate is that the phosphocline is persistently deeper than nitracline, leading to supra-Redfield N:P ratios in the 100-140m depth interval of the mean state. Both cyclones and MWEs tend to upwell that stratum in their formation and intensification phase. Enhanced mixing in MWEs could result in N:P ratios much closer to Redfield in the upwelled waters. However, at-sea nutrient measurements by Qian Li indicate phosphate concentrations at the base of the euphotic zone in C5 actually exceed those in A4 (Figure 0626.3), thereby indicating that phosphate is not the key variable responsible for the difference between blooms in cyclones and MWEs. Perhaps other nutrients could be regulating the response. Silicate measurements will be made on frozen samples, and those data will be available this fall. Iron is also an interesting possibility. Sedwick et al. (2005) document the iron profile inside a cyclone in May 2004, the feature (C1) that was later chosen as the target for sampling in the EDDIES program. The iron profile exhibits a subsurface minimum at the base of the euphotic zone, presumably due to biological uptake. Concentrations increase both toward the surface (Aeolian input) and in the deeper layers (remineralization of sinking particles). If the Sedwick profile is typical, then enhanced mixing inside MWEs would tend to increase iron supply from both above and below, potentially stimulating a bloom of diatoms. Iron measurements are clearly needed in an MWE to test this hypothesis.

8. Cruise Narrative

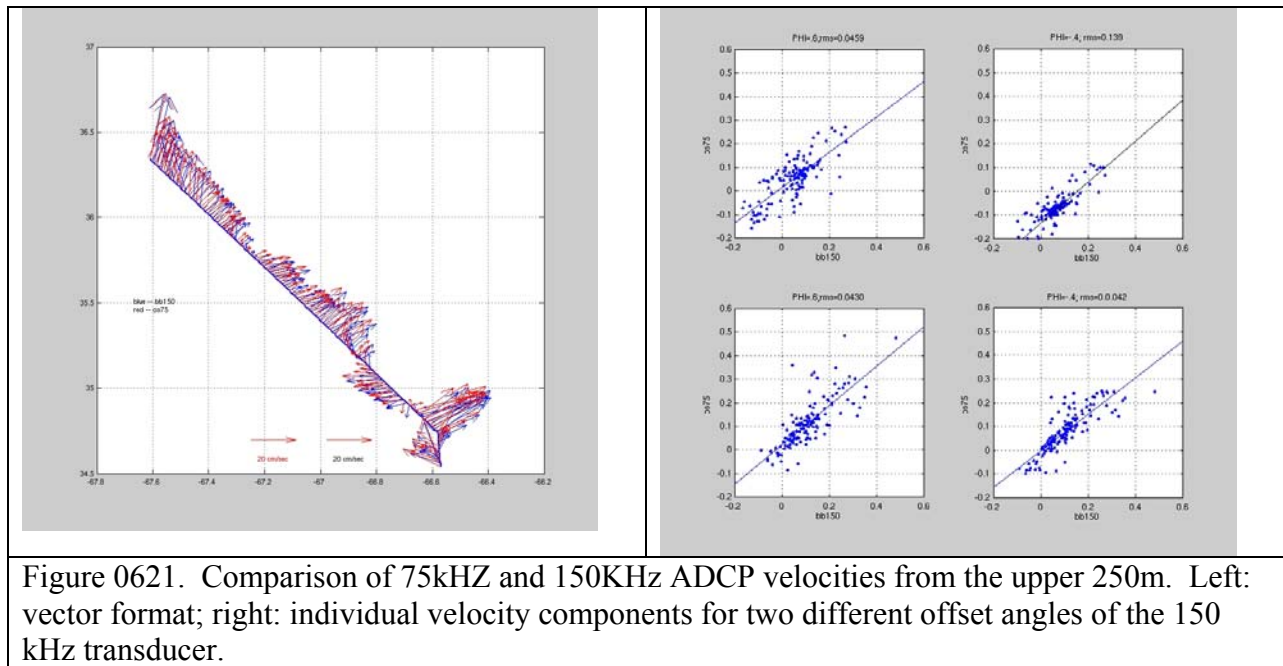
June 20

Departure at 1015. Underway sampling of *Alexandrium fundyense* from Vineyard Sound out to the shelf break. Two CTD casts for training purposes.

June 21

Transit continues. Test CTD #3, XBT #1, and light probe.

OS75 and 150KHz ADCPs were run simultaneously for a brief period for intercomparison purposes. Velocities obtained from both instruments were averaged in the upper 250m. Both instruments reveal similar mesoscale structure in the velocity field (Figure 0621.1 left panel). Individual velocity components are compared in the right panel using a previous estimate of the 150KHz unit's transducer offset angle (-0.4 degrees) and a refined estimate from OC412 (Ruoying He). Good quantitative comparison is achieved when the updated offset angle is used. Offset angle for the OS75 is 41.5 degrees, as per RDI on-board calibration.



June 22

XBT/ADCP search for C5 center begins. Sighted a pair of sperm whales basking on the surface. Initial N-S section cuts right through eddy center, with velocity going to zero, and clear doming

of the main thermocline peaking at XBT # 15 (Figure 2). CTD at waypoint #3024 indicates this is clearly not a cold-core ring, as its temperature and salinity characteristics match those of a mid-ocean eddy (21, 36.6; 20, 36.6; 19, 36.6; 18, 36.6; 16, 36.2).

MOCNESS tow indicates low biomass overall, with the caveat that the nets were partially tangled. Low biomass of migrators corroborated by surface net tows. Lots of *Trichodesmium* tufts in the 200-300m depth interval.

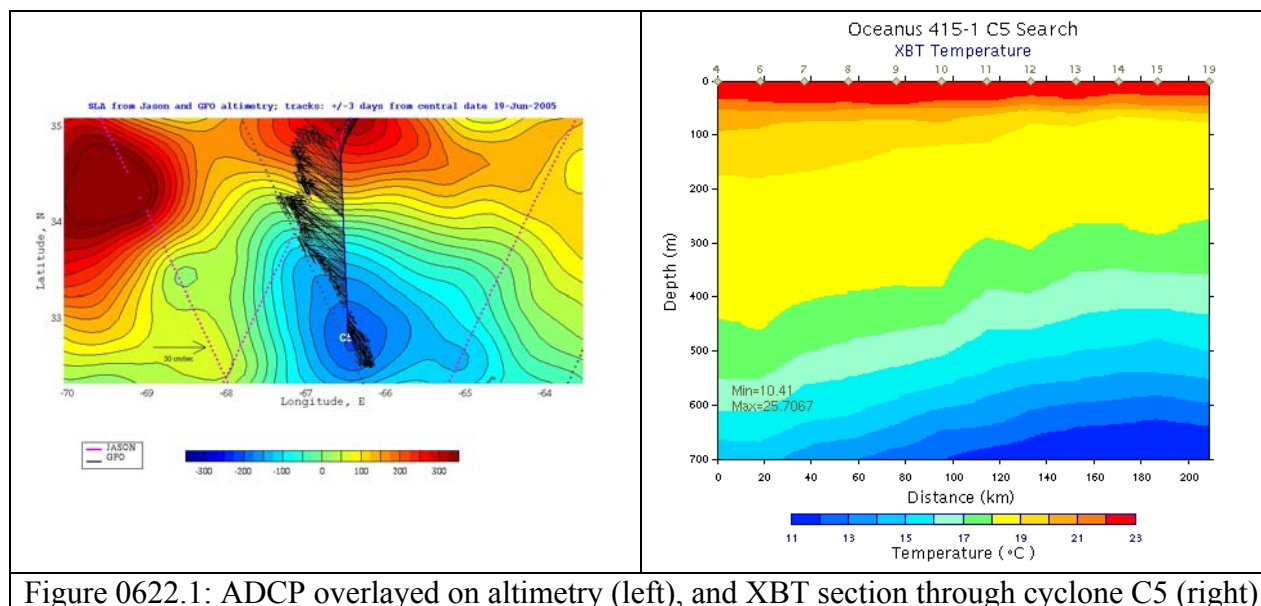


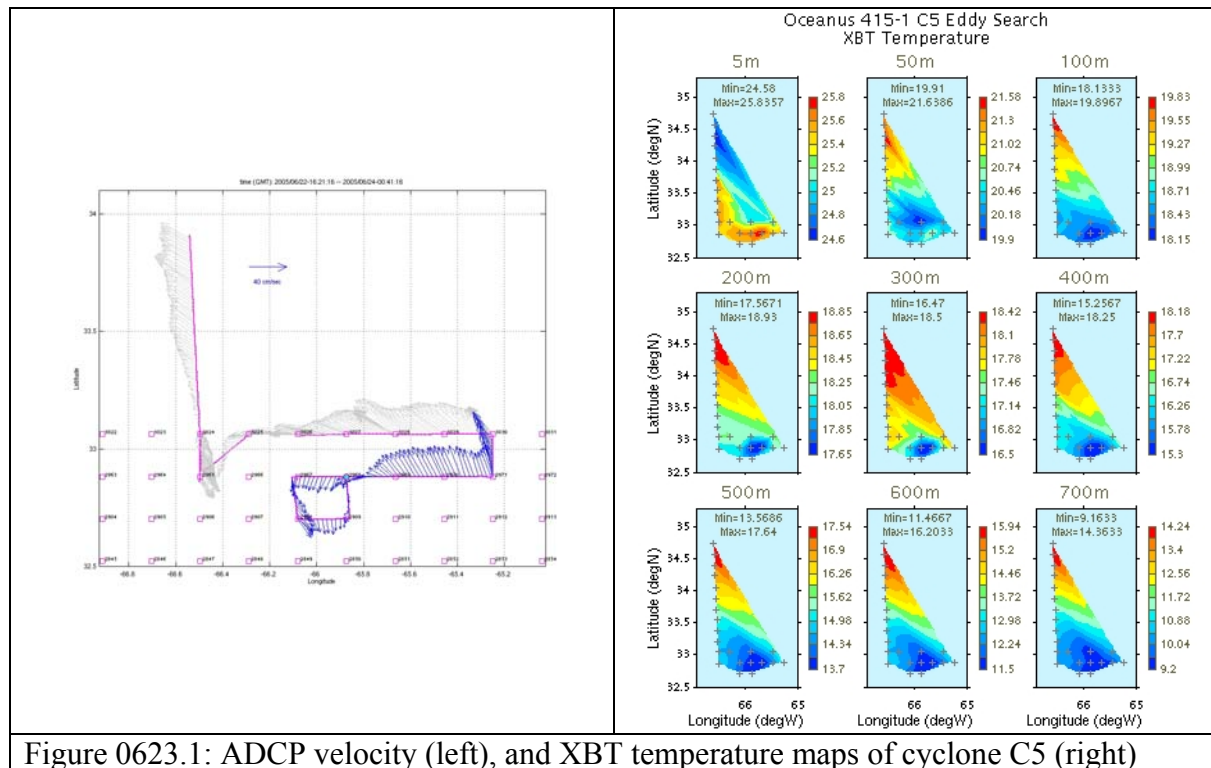
Figure 0622.1: ADCP overlaid on altimetry (left), and XBT section through cyclone C5 (right)

June 23

ADCP and hydrographic structure indicates we were not in the center of C5 (Figure 0623.1). Colder temperatures were evident in the 50-700m depth interval as we proceeded eastward along the XBT/CTD transect (XBT stations 20, 21, 22; CTD stations 4, 5, 6, 7; see Figure 0623.2). ADCP velocities revealed that the low velocity core originally thought to be eddy center was associated with a distinct cyclonic feature to the west of C5. Subsequent to completion of the 4th CTD in the line, we recommenced an XBT/ADCP survey to relocate eddy center. A local minimum in temperature together with near-zero velocity was found at waypoint # 2968. An additional CTD was conducted at that location, facilitating a cross-eddy transect to be compiled with stations 4-5-9-6-7 (Figure 0623.3). Eddy center (station 9) is displaced 20 km south of the original east-west line, but that does not preclude assembly of the transect.

Uplift of the seasonal and main thermoclines is clearly evident in the center of the eddy. Salinity and oxygen isopleths are similarly displaced. The cold temperature anomaly at 100m is approximately 1°C. Interestingly, the layer of 18°C water thins considerably at eddy center, and that is accompanied by an oxygen deficit in the waters below. Clearly there are problems with the fluorescence data, as the background levels measured in deep water are highly variable.

MOCNESS tow at eddy center reveals high migrator biomass in the near-surface waters; catches in the deeper layers were relatively modest. Trichodesmium was abundant in the 150-300m depth interval.



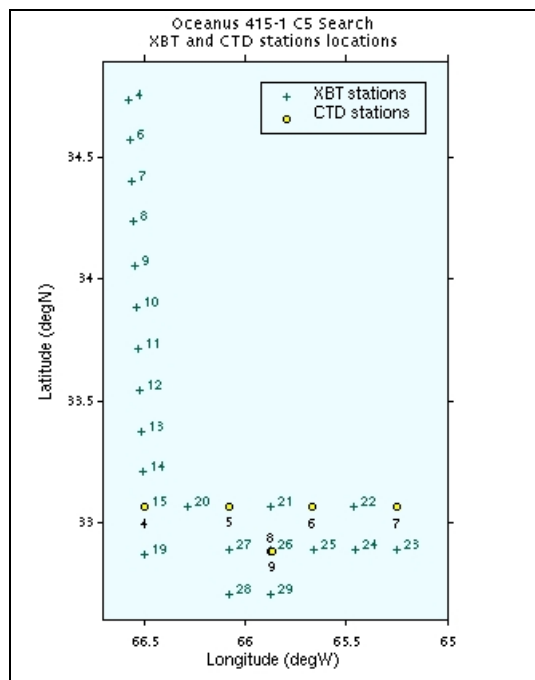


Figure 0623.2: Station locations for the initial survey of C5.

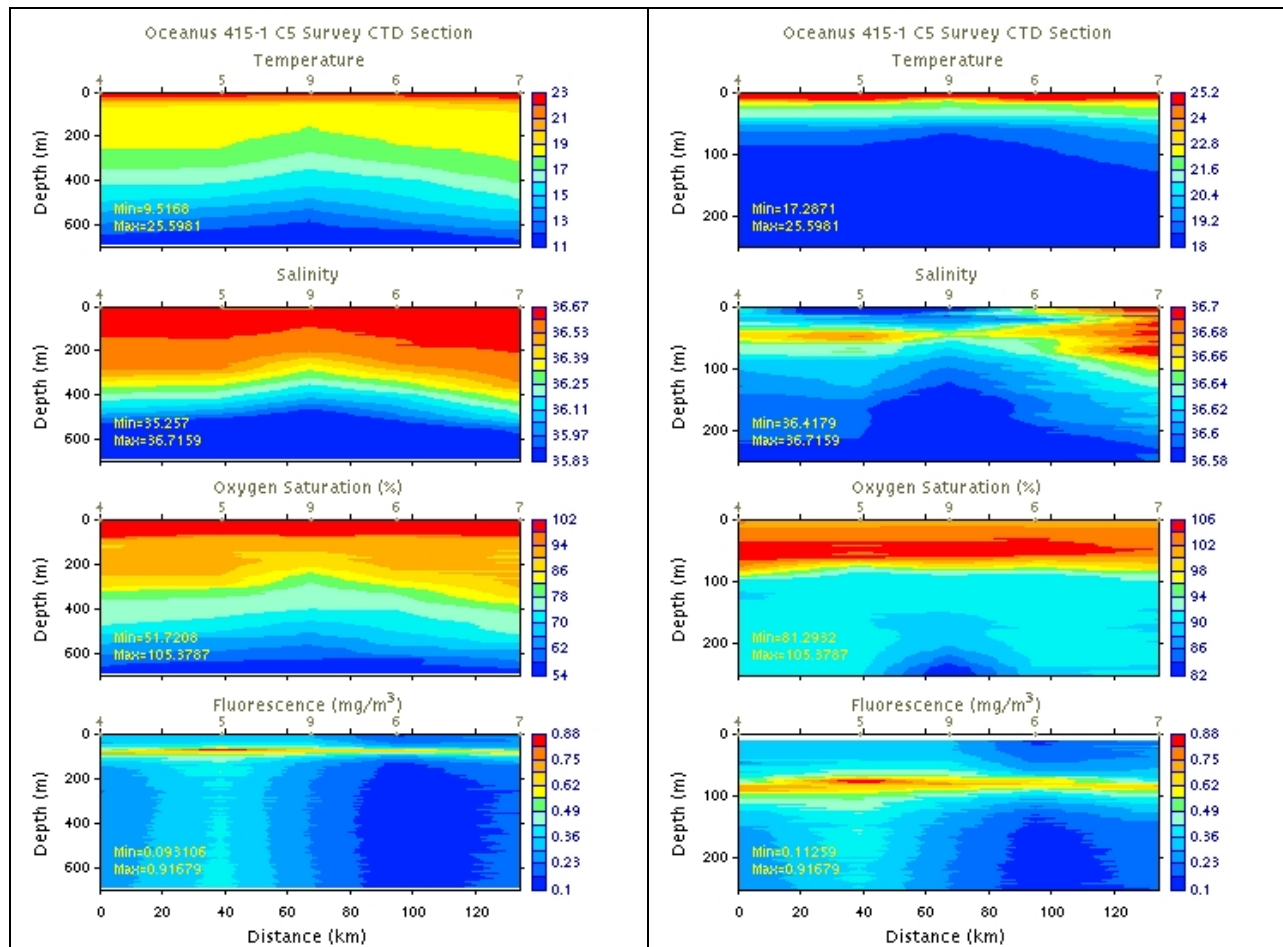


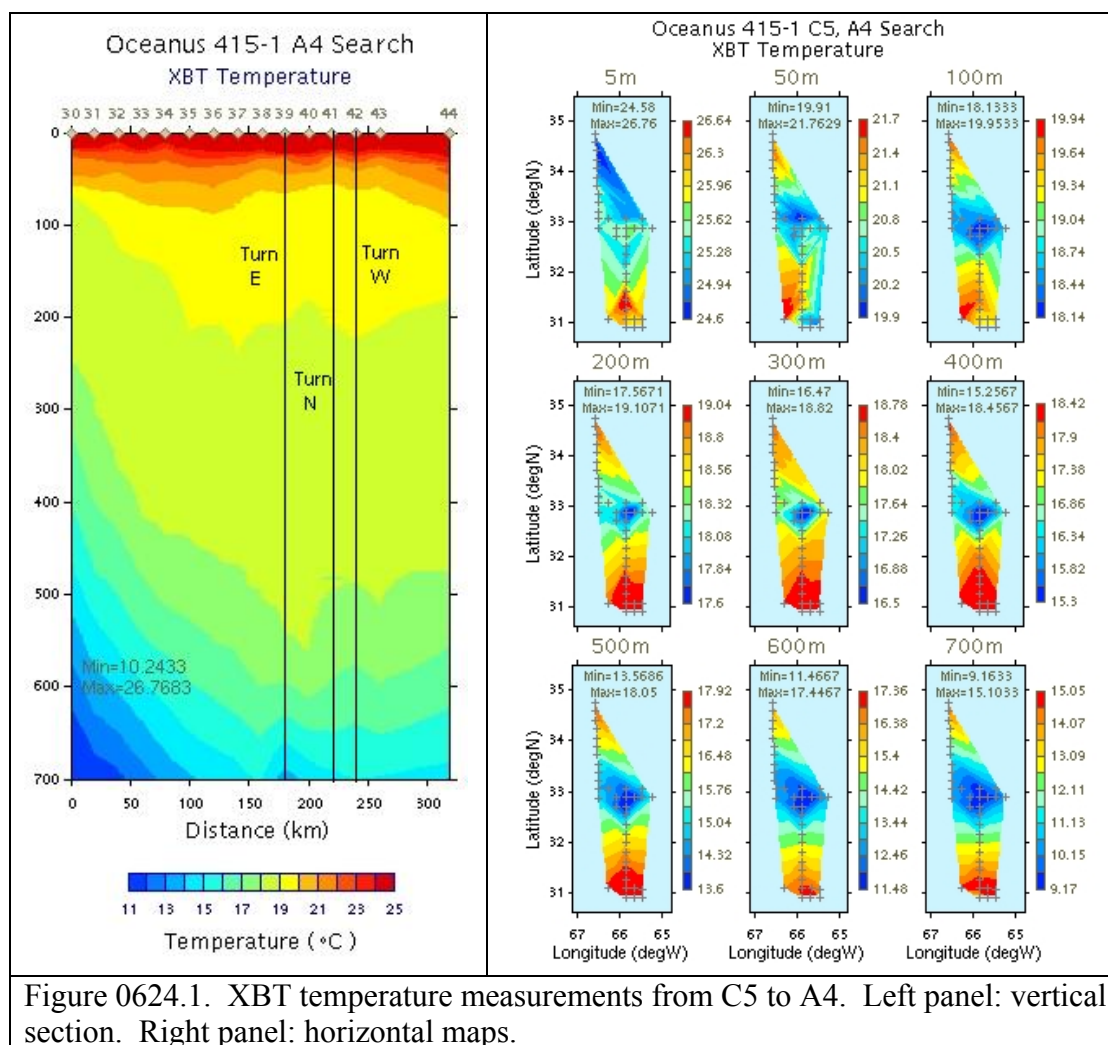
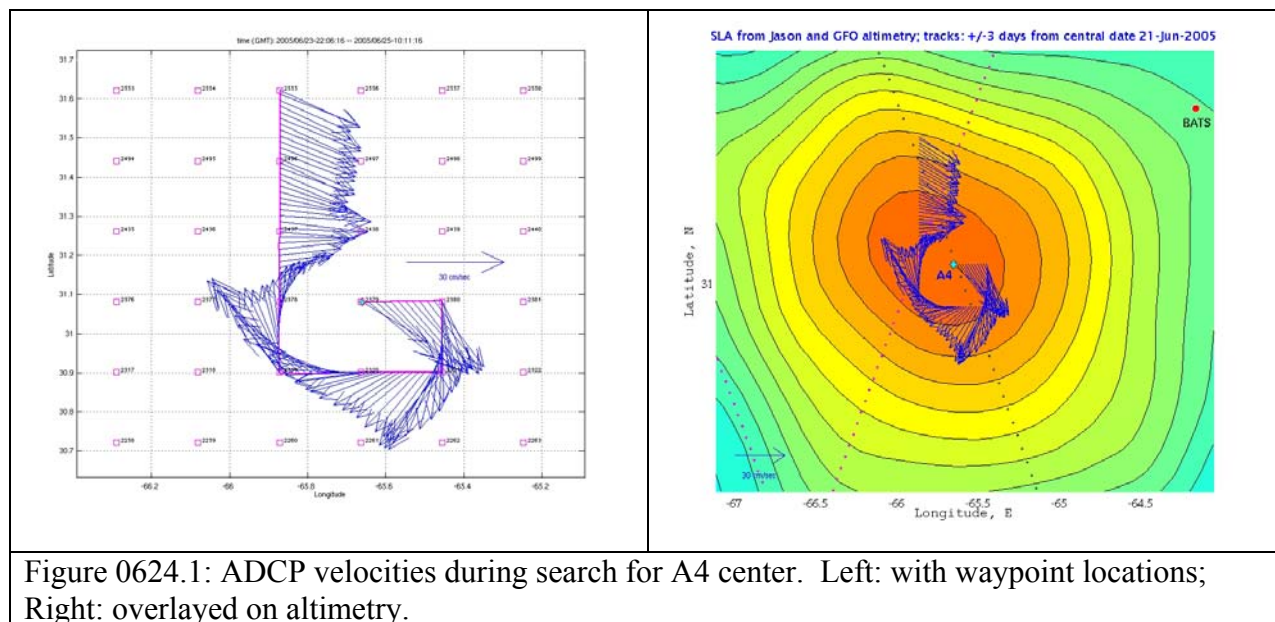
Figure 0623.3: Temperature, salinity, oxygen saturation, and fluorescence across cyclone C5. Left: 0-700m; Right: 0-250m. Note fluorescence data are suspect.

June 24

VPR deployed for survey of C5 and transit to A4. Flight control problems required recovery of the vehicle. Transit toward A4 begins with underway XBT/ADCP survey.

Anticyclone A4 exhibits a classic velocity structure with high lateral velocity shear near the center (Figure 0624.1). The 20km station grid clearly delimited eddy center, but did not resolve the exact center with near-zero velocity. The sea level anomaly field for A4 is well constrained by two ground tracks crossing near its center; correspondence between the ADCP velocities and the SLA field is near perfect.

The alongtrack XBT section reveals a precipitous drop in the main thermocline from the interior of C5 to the interior of A4 (Figure 0624.2, left panel). Temperature at 700m in the cores of the two eddies differs by nearly 6°C (Figure 0624.2, right panel). The seasonal thermocline domes slightly in the interior of A4 such that temperatures in the upper 100m are slightly cooler in the core of A4 than in the periphery. However, the upper ocean temperature anomaly in A4 is not nearly as strong as in C5.



MOCNESS tow at the center of A4 indicated high biomass overall. Migrator biomass was high in the upper 200m, and was higher than the other tows in the 200-300m depth interval. Large sergestid shrimp were noted in that stratum.

June 25

CTD section of A4 completed (Figures 0625.1, 0625.2). At 700m, the main thermocline was deepened by more than 100m at eddy center. Modest uplift of the seasonal thermocline was also evident in the core of the eddy. Although problems persist with the fluorometer, it is clear that the subsurface fluorescence maximum is higher in the water column and enhanced with respect to the eddy periphery.

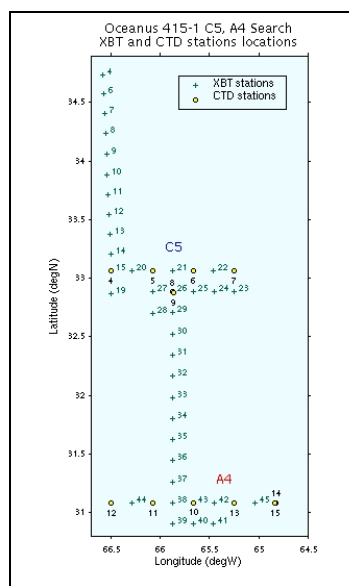


Figure 0625.1: Station locations for the initial surveys of C5 and A4.

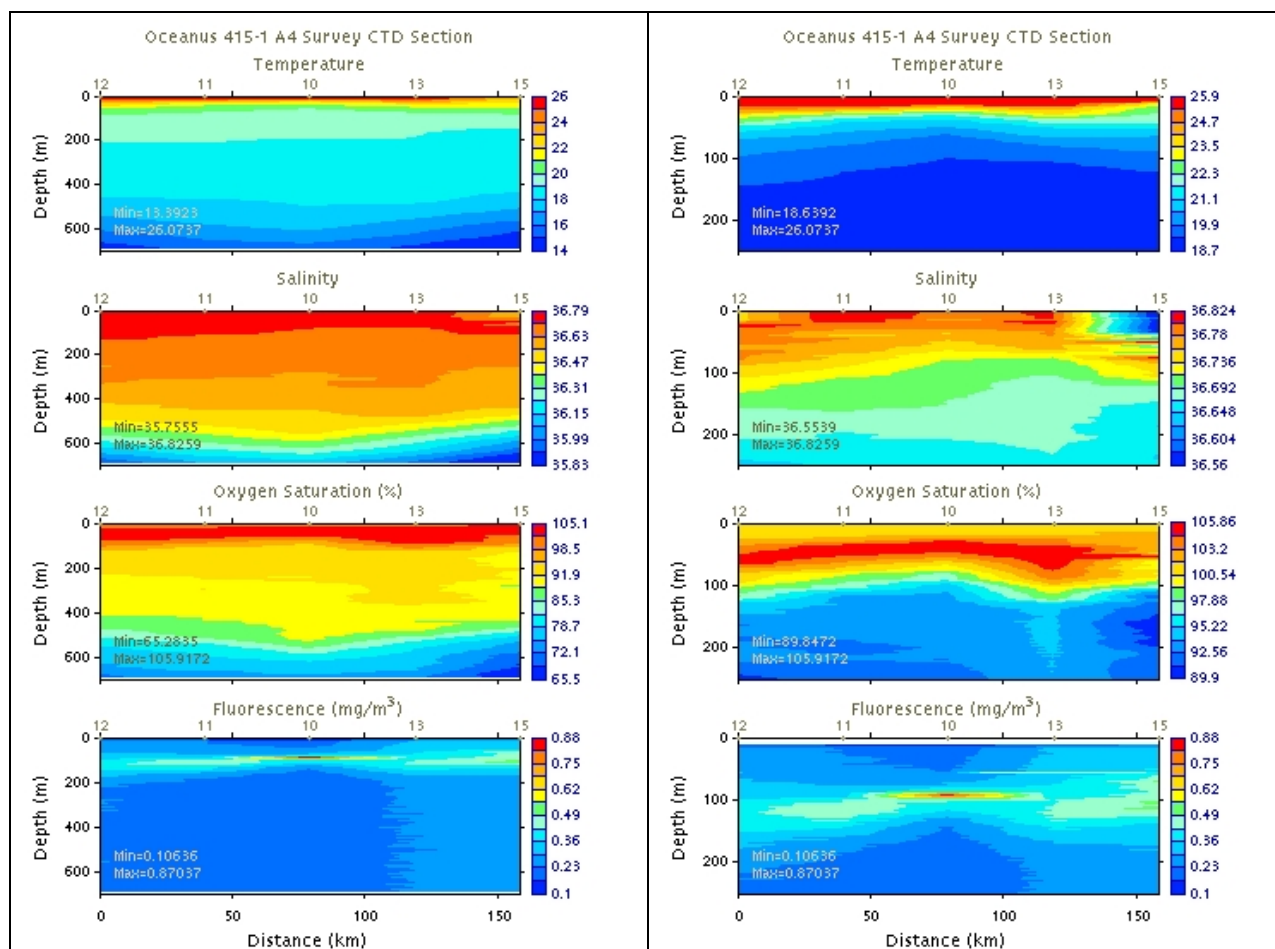


Figure 0625.1: Temperature, salinity, oxygen saturation, and fluorescence across anticyclone A4. Left: 0-700m; Right: 0-250m. Note fluorescence data problems are less severe except in the easternmost two stations (13 and 15).

June 26

VPR transects through A4 (Figure 0626.1) reveals the structure of the high fluorescence patch at eddy center, with some values more than a factor of two higher than in the CTD trace (Figure 0625.1). VPR data were used to locate an additional CTD cast in the middle of fluorescence patch. This special cast consisted of 8 depths (surface, 40, 60, 80, 100, 120, 140, fluorescence max) with 3 niskins each so that live cell counts and DNA samples could be taken in addition to the normal suite of measurements.

The cast revealed a thin layer of high fluorescence, with peak values at 106m of approximately $2.9 \mu\text{g Chl a l}^{-1}$ recorded on the CTD fluorometer (Figure 0626.2). Pigment extraction from the niskin bottle at that depth confirms high chlorophyll, with the BATS team (Megan and Christine) reporting values of 1.379 and 0.646 for chlorophyll a and phaeophytin, respectively. Tom Bibby reported FRRF results indicating that the >10 micron size fraction constituted the majority of the chlorophyll in that layer. However, even the smallest size fraction (< 1 micron) was had more

chlorophyll at 106m than any other depth. Thus, both small and large size fractions appear to be responding to the increase in nutrients at the base of the euphotic zone.

Microscopic analysis of the live sample from the chlorophyll maximum revealed an extraordinary abundance of diatom chains. Concentration was estimated to be 8000 chains per liter based on counts by Kevin Wyman.

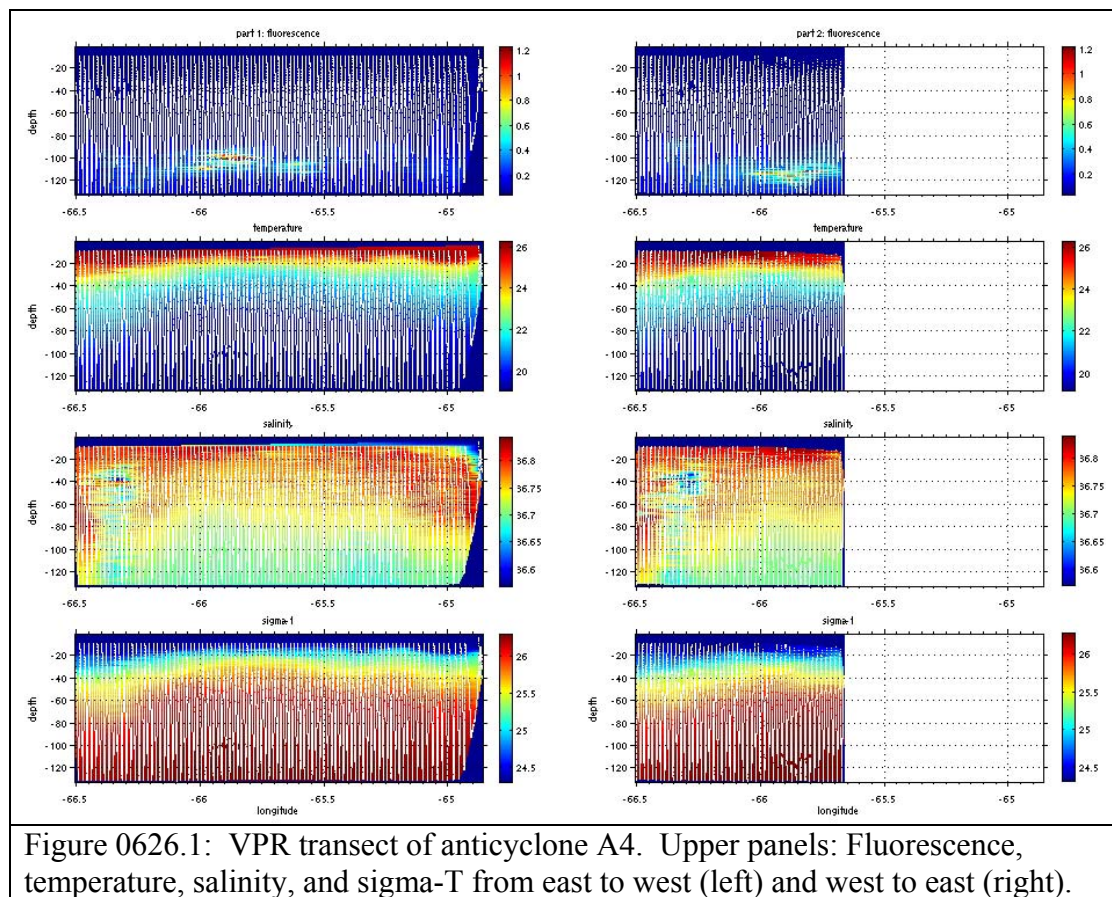
Nutrient measurements from Qian Li indicate dissolved inorganic nitrogen is enhanced at the base of the euphotic zone in the core of A4, with concentrations of approximately 0.5 μM at 90m, and 1.0 μM at 100m (Figure 0626.3). Dissolved inorganic phosphorus shows a similar pattern of enhancement at eddy center, with concentrations of approximately 0.1 μM at 100m.

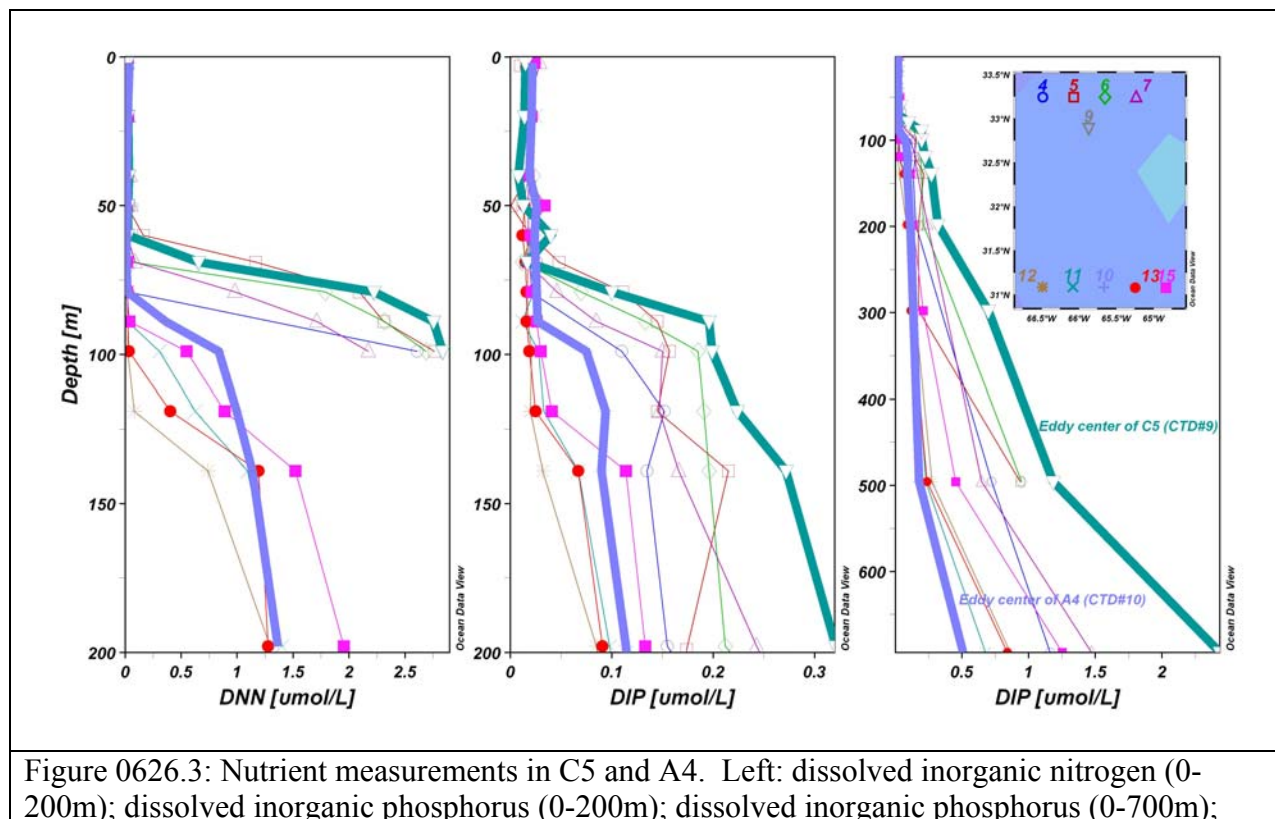
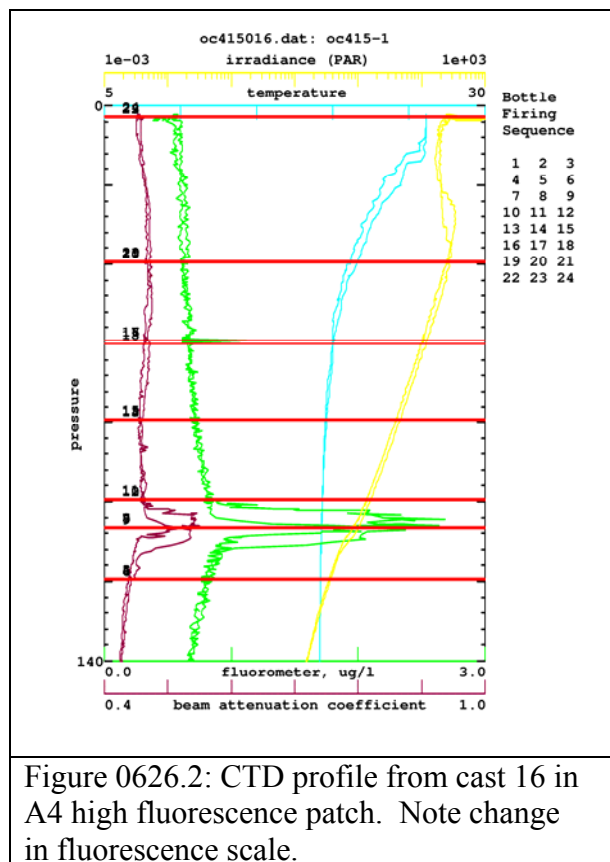
Live counts: 87 chains in 1 swipe at 20x. 2 liters filtered. Washed into 13ml.
Normal multiplier for 2 swipes, 20x, 6 liters filtered, 10 ml tube.

Concentration estimate: $87 \times 2 \text{ swipes} \times (6 \text{ liters} / 2 \text{ liters}) \times (13 \text{ ml} / 10 \text{ ml}) \times 12 = 8143$ chains per liter.

Another curious feature revealed by the VPR data is the patch of low salinity water on the western side of the eddy (Figure 0626.1). This structure is clearly not instrumental artifact, as it is present in both the east-to-west and west-to-east transects. It has no apparent impact on stratification (lower panels) or Brunt-Vaisala frequency (not shown). Interestingly, a similar feature was detected on the eastern side of the eddy (Figure 0625.1, station 15). We presume that this was not detected by the VPR because the instrument was not deployed until the ship had moved west of station 15. Both the eastern and western salinity anomalies have similar T-S characteristics (Figure 0626.4). What is the origin of these anomalies? The density structure and T-S curves are not consistent with a mixing event. The salinities, while low relative to that in the interior of the feature, are within the envelope of “ambient” conditions for this area (see T-S plot from CTD data in 2004). Thus it seems most likely that these features are streamers along the periphery of the eddy that are entraining water laterally. Eddy-scale mapping will be necessary to determine their detailed structure and origin.

VPR redeployed for transit from A4 center to C3. Intermittent data dropouts require recovery. Fiberoptic connectors to the VPR can were found to be loose and partially flooded. Connectors cleaned and VPR redeployed.





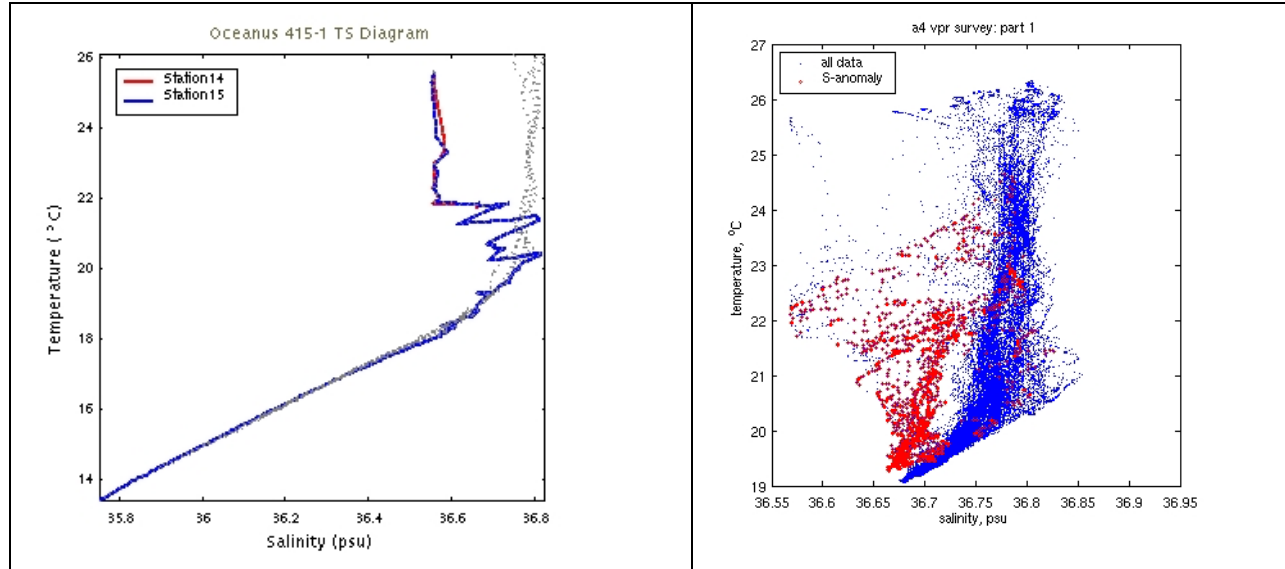


Figure 0626.4: Temperature and salinity characteristics for CTD stations (left) and the VPR transect across A4 (right). Stations 14 and 15 are colored in the left hand panel to identify the salinity anomaly on the eastern side of A4. In the right hand panel, VPR data points between -66.4 and -66.3°W and greater than 30m depth are plotted in red to identify the salinity anomaly on the western side of A4.

Details of CTD 16 – A4 Chlorophyll patch

Depths: surface, 40, 60, 80, 100, 120, 140, chl max somewhere in between

Depth #1

1,2 – regular BATS sampling + size fractionated FRRF + flow cytometer
3 – live count + DNA

Depth #2

4,5 – regular BATS sampling + size fractionated FRRF + flow cytometer
6 – live count + DNA

Depth #3

7,8 – regular BATS sampling + size fractionated FRRF + flow cytometer
9 – live count + DNA

Depth #4

10,11 – regular BATS sampling + size fractionated FRRF + flow cytometer
12 – live count + DNA

Depth #5

13,14 – regular BATS sampling + size fractionated FRRF + flow cytometer
15 – live count + DNA

Depth #6

16,17 – regular BATS sampling + size fractionated FRRF + flow cytometer
18 – live count + DNA

Depth #7

19,20 – regular BATS sampling + size fractionated FRRF + flow cytometer

21 – live count + DNA

Depth #8

22,23 – regular BATS sampling + size fractionated FRRF + flow cytometer

24 – live count + DNA

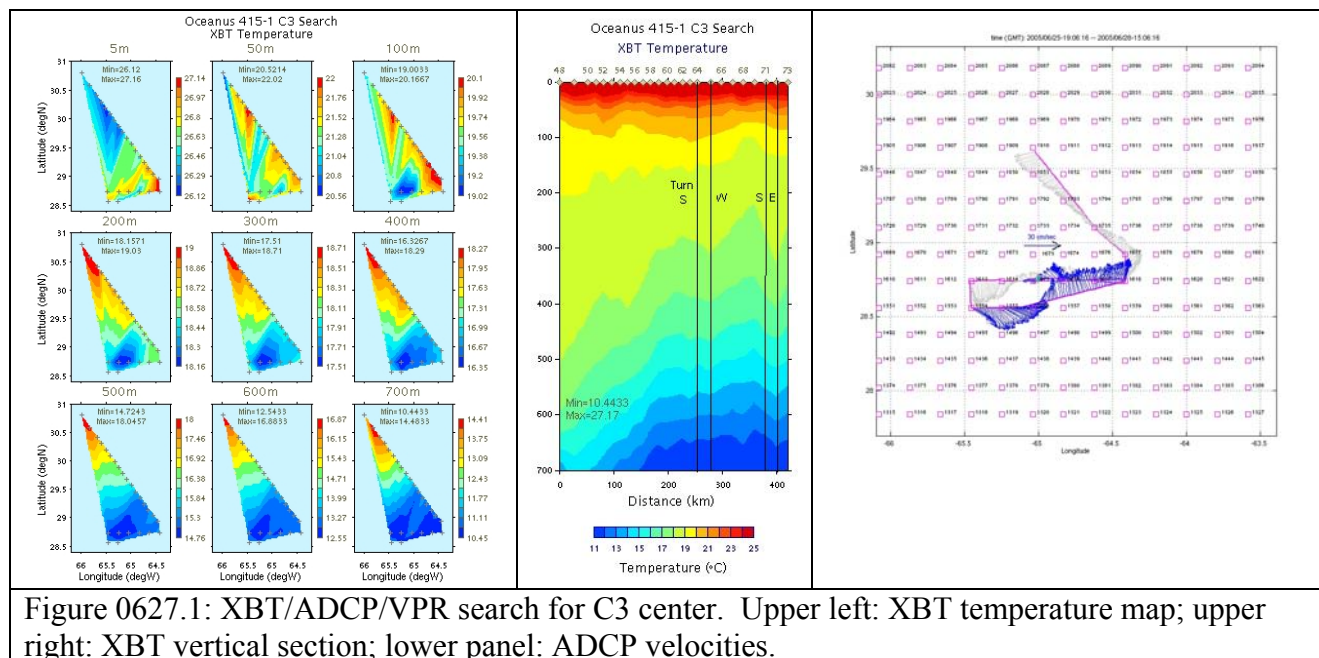
FRRF samples size fractionated at 10,5,3,1 microns

Live count: 8 liters, 10 micron mesh

DNA: 2 liters

June 27

VPR transect to C3 continues. Center of C3 located at waypoint #1614 (Figure 0627.1), ca. 40 miles SE of its last known position ca. 1 week prior.



June 28

CTD Section of C3 completed (Figures 0628.1 and 0628.2). C3 shows classic characteristics of eddy-induced upwelling in its core: doming of the seasonal thermocline, enhanced fluorescence, and a positive oxygen anomaly in the overlying waters. Qian Li's data indicate nutrient enhancement at eddy center, with 90m nitrate and phosphate concentrations of 1.0 and 0.05 μM respectively (Figure 0628.3).

MOCNESS tow at eddy center had low biomass overall (caveat: nets tangled), similar to the periphery station of C5. The only difference was the presence of large migrators in the 0-100m depth interval in C3.

Incubation cast at eddy center (Nemmergut and Bibby).

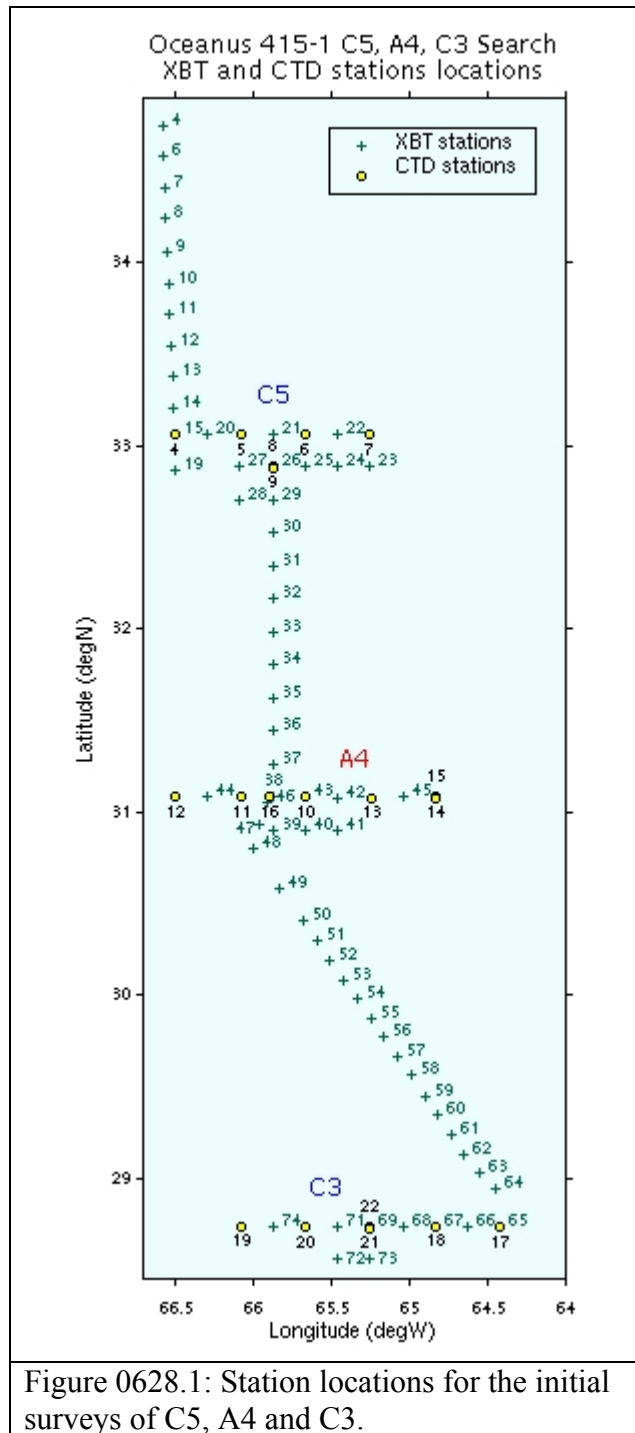
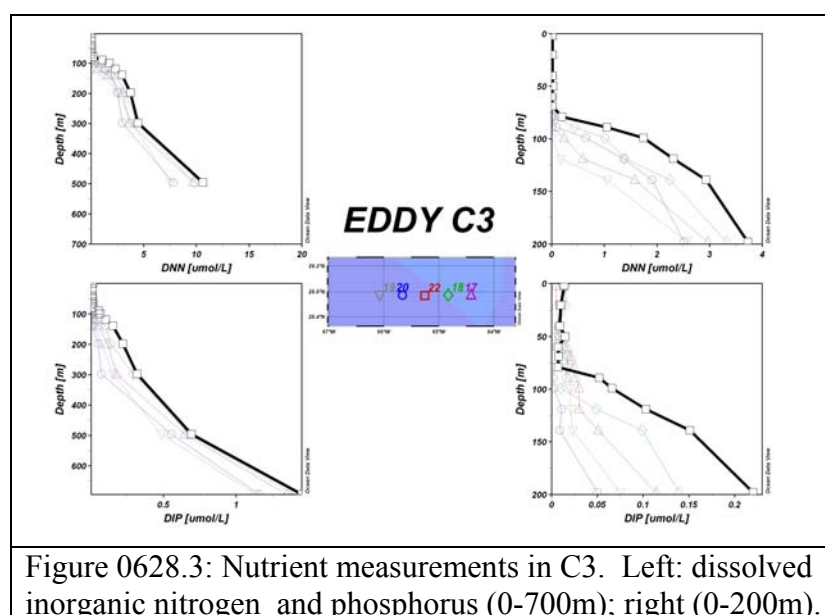
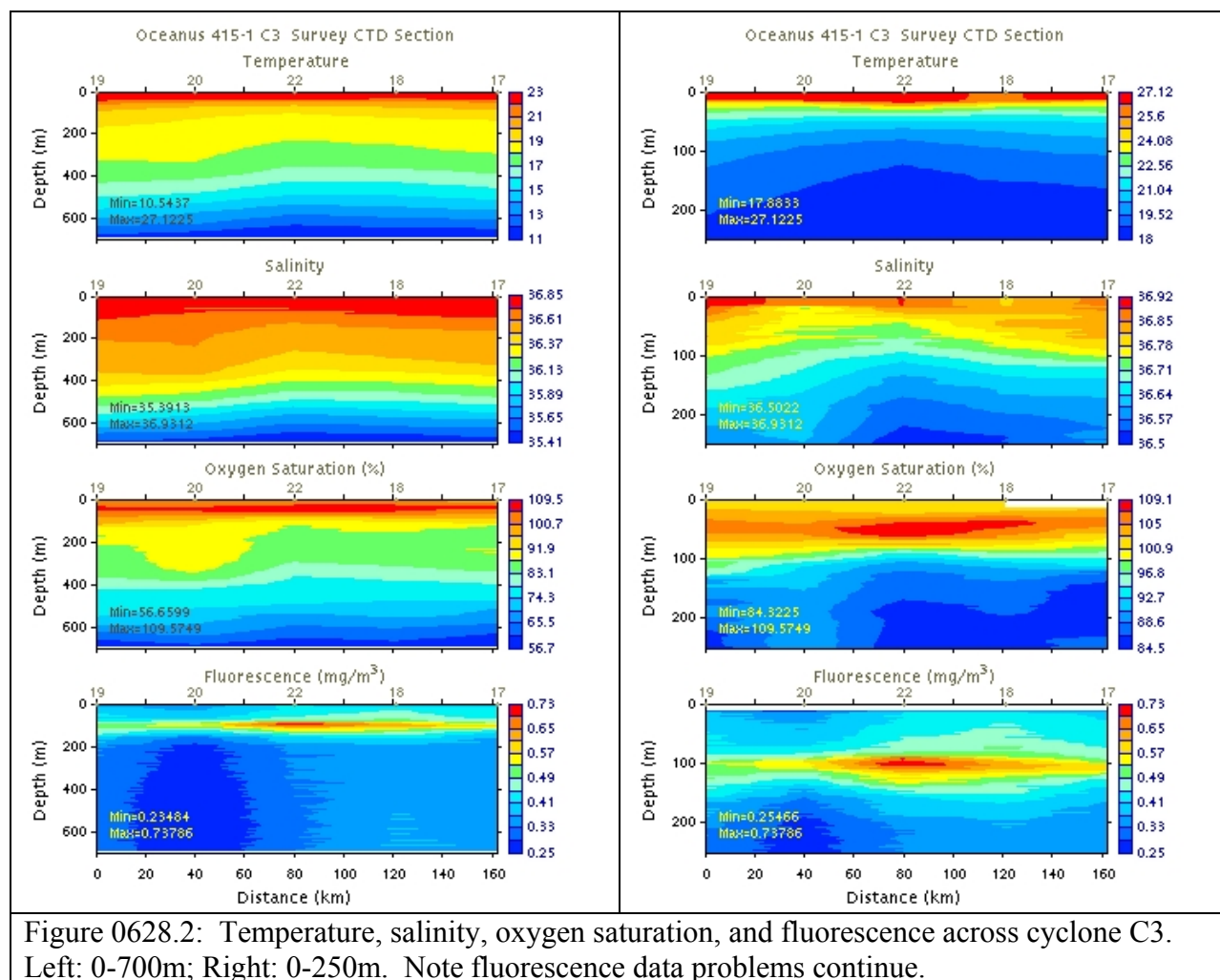
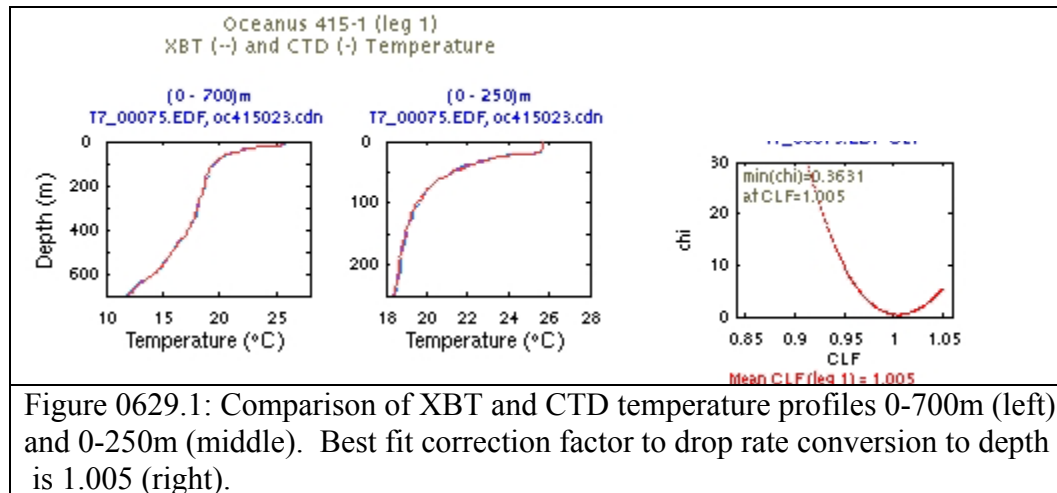


Figure 0628.1: Station locations for the initial surveys of C5, A4 and C3.



June 29

Transit to BATS for MOCNESS and CTD cast. XBT launched at CTD station for calibration purposes (Figure 0629.1). Drop rate equation appears robust, as best fit between CTD and XBT temperature is to adjust XBT depth by a factor of 1.005.



MOCNESS tow at BATS yields overall biomass that is comparable to the two cyclones already sampled. Euphausiids were abundant in the upper 100m, yet the waters deeper than 500m had the lowest biomass of any tow.

Slow transit to Hydrostation S to await WBII.

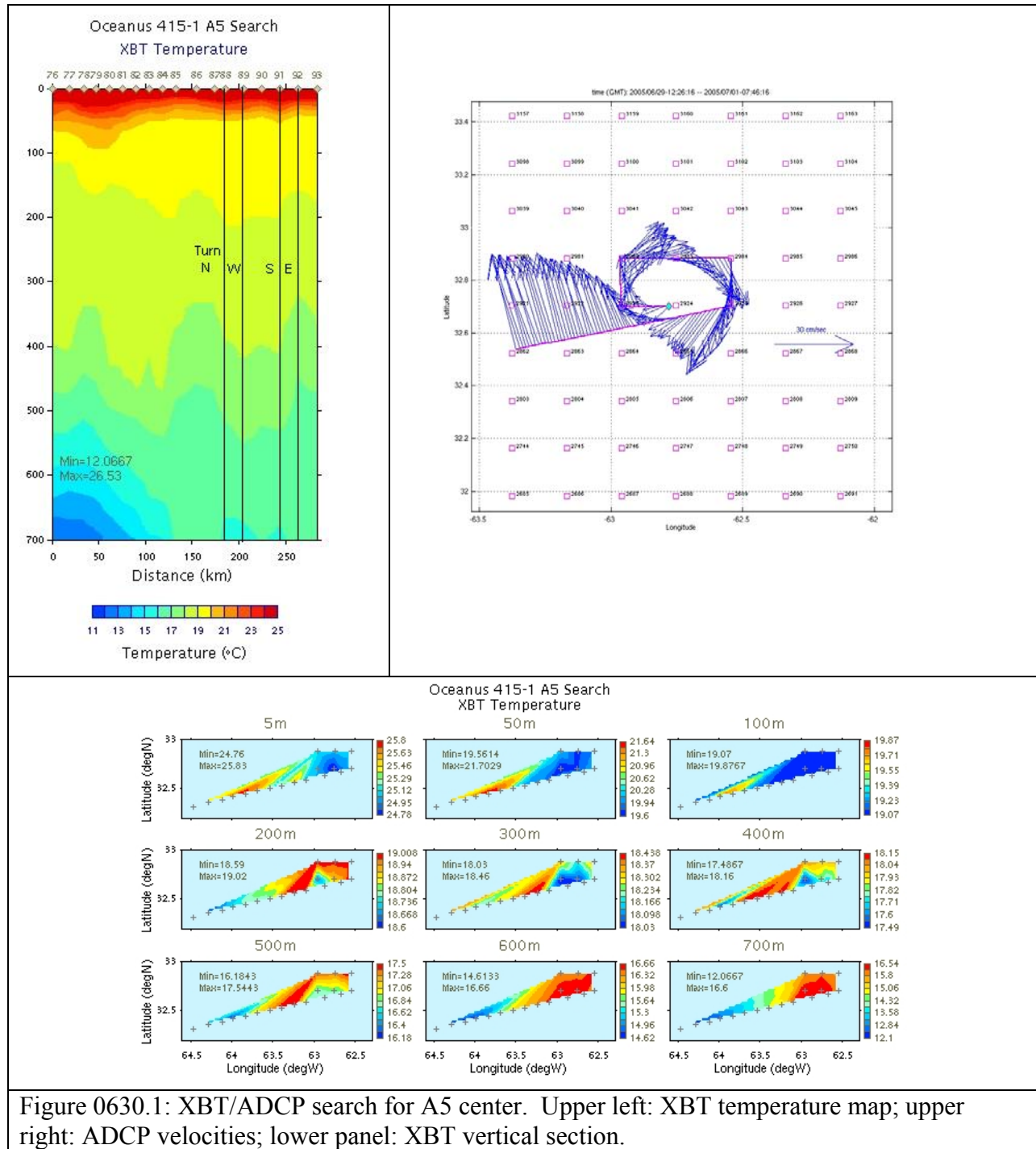
June 30

Rendezvous with WBII for fluorometer dropoff. Transit toward A5 begins. VPR deployed and immediately recovered due to dropouts of flight control data. Connector tightened and redeployed, worked OK for a few hours before dropouts reappeared. Fish recovered immediately.

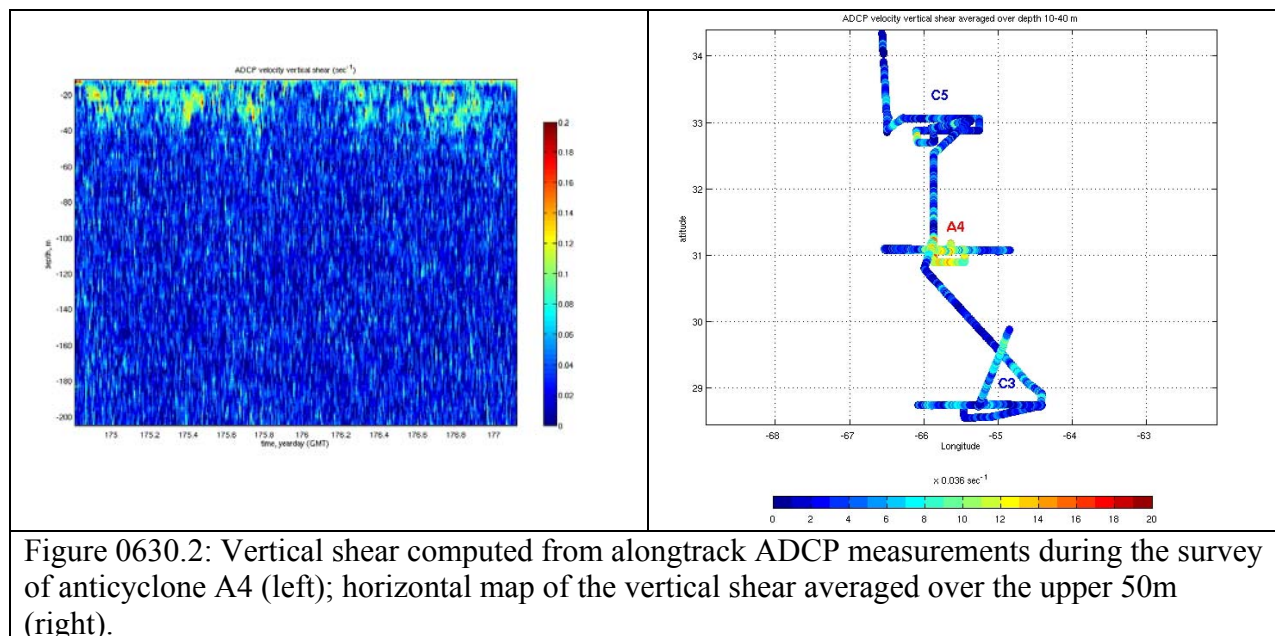
Search of A5 center with XBT/ADCP only (Figure 0630.1). Temperature structure indicates the presence of a 16° mode-water eddy, reminiscent of A1 from 2004.

New fluorometer installed in CTD package. OBS and altimeter and Y-cable removed from voltage 2, 3. New fluorometer on voltage 3, defined as user polynomial 0. Coefficients a_0 and a_1 calculated as per manual, using highest sensitivity setting set in firmware by Dave M.: $a_0 = -\text{scale factor} * V_{\text{blank}} = -.642$; $a_1 = \text{scale factor} = 6.0$. Prior configuration file saved as oc415-1_old_fluorometer.con.

Old fluorometer kept on frame for intercomparison purposes.



Vertical shear calculations from the ADCP indicate that largest shears are confined to the upper 50m (Figure 0630.1, left panel). These appear to be associated with inertial motions that are enhanced in the interior of anticyclone A4 (Figure 0630.2, right panel). Trapping or focusing of near-inertial motions may play a role in generating mixing that leads to enhanced productivity in the cores of anticyclones.



July 1

CTD survey of A5 completed (Figure 0701.1), confirming the 16° mode-water eddy structure (Figure 0701.2). A 1500m cast was carried out at eddy center to examine the deeper structure and capture the base of the main thermocline. Profiles are strikingly similar to eddy A1 observed in 2004 (Figure 0701.3). Nutrient measurements from Qian Li indicate nutrient enhancement (reduction) in near-surface (deep) waters (Figure 0701.4), consistent with a mode-water eddy displacements to the seasonal and main thermoclines, respectively.

MOCNESS tow at eddy center yields highest biomass yet; incubation casts for Bibby/Nemmergut; VPR deployed for E-W transect of A5.

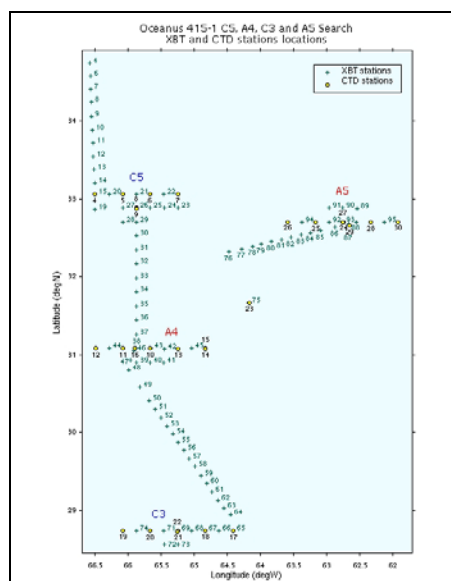
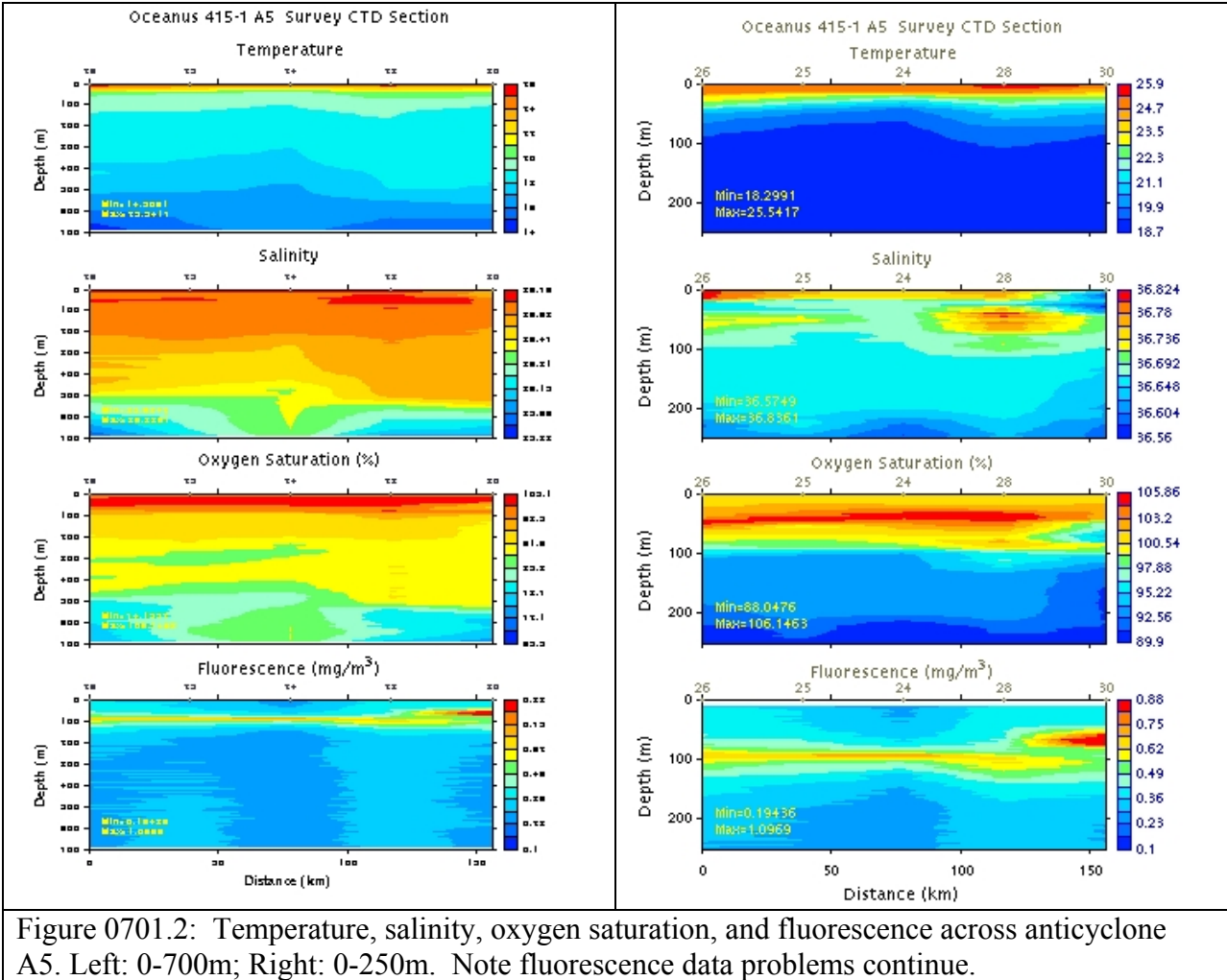


Figure 0701.1: Station locations for the initial surveys of C5, A4, C3 and A5.



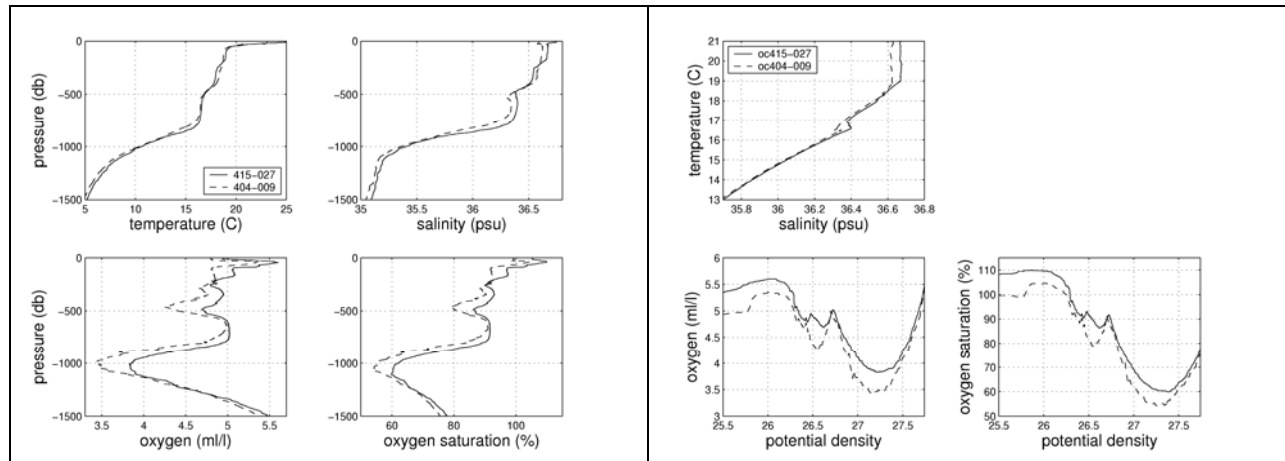


Figure 0701.3: Temperature, salinity, and oxygen characteristics of A5 compared to those of A1 sampled in 2004.

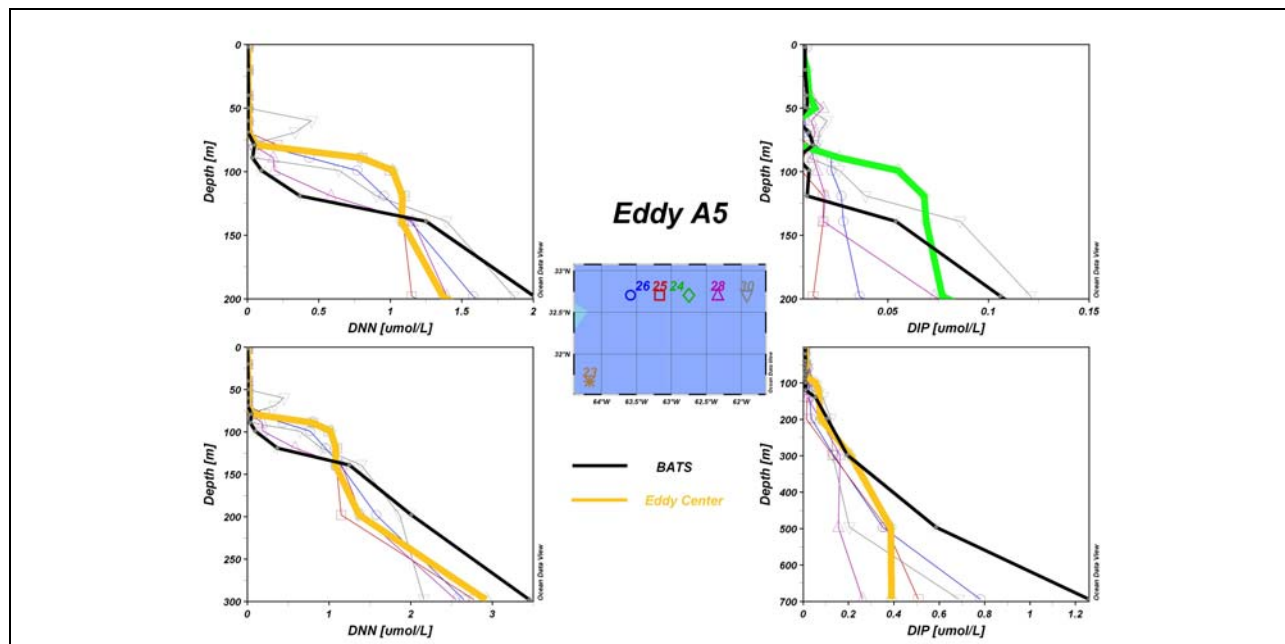


Figure 0701.4: Nutrient measurements in A5 as compared with BATS. Left: dissolved inorganic nitrogen (0-200m and 0-300m); right: dissolved inorganic phosphorus (0-200m and 0-700m).

July 2

A science meeting was held to discuss the choice of a target eddy from among the four that were sampled in the first phase of the cruise. All four eddies have appealing characteristics and would make fine subjects for future study (Table 1). Our choice of the target eddy was based on the evidence we had in hand for the various aspects of the physical-biological-biogeochemical dynamic of interest: an eddy-induced nutrient supply leading to a physiological response in the

phytoplankton, a change in species composition, and a change in export flux and biogeochemical cycling. Our observations pertain to the first three aspects; export flux will not be measured until the joint operation with R/V *Weatherbird II* begins.

Nutrient enhancement was evident in all four eddies, as was a physiological response in the phytoplankton community. Changes in phytoplankton species composition and community structure were most evident in anticyclones A4 and A5. However, the prospect that A5 is a relatively rare type of eddy with a distant origin leads to some concern over the degree to which we would be able to generalize the results from a detailed study of that feature. Moreover, the apparent trapping of near-inertial motions and higher vertical shears observed in A4 makes it a compelling candidate for study of mixing processes in the tracer release component of the project led by Jim Ledwell. Therefore A4 was chosen as the target feature. That being said, we hope to revisit one or more of the other features as time permits.

	Physics	Nutrients	Oxygen	Chl+Phaeo (CTD/VPR / Turner)	FRRF	MOCNESS (Biomass Rank)	Surface tows
C 5	Cyclone	1 Very high nutrients in eddy core: >2µM NO ₃ at 80m	EZ O ₂ anomaly delimited to east, not to west. O ₂ deficit possibly developing at depth	2 1.0/-1.1	High Fv/Fm values in Chl max; patchy signal in upper water column. Chl max slightly elevated at eddy center to 80m. Phytoplankton community dominated by <3µ size class.	(3) Periphery: low biomass, few migrators, Tricho present 150-300m. Center: many small (1- 2mm) euphausiids, very low biomass >200m.	Periphery: many small euphausiids and fish larvae Center: small euphausiids
A 4	Mode Water Eddy Weak displacement of seasonal thermocline; high shear in upper ocean	4 Enhancement in eddy core: 0.5 µM NO ₃ at 90m 1.0 µM NO ₃ at 100m	EZ O ₂ anomaly delimited to east, not to west.	1 2.9/2.5/2.0	High Fv/Fm values following the Chl max. Chl max enhanced at eddy center where the phytoplankton community is dominated by >10µ size class; identified as chains of diatom <i>Chaetoceros</i> spp. (approx 8000 chains / l)	(2) Second highest biomass in upper 300m all size fractions; many medium euphausiids and some sergestid shrimp	Many colonial radiolarians and small copepods.
C 3	Cyclone	2 Enhancement in eddy core: 1.0 µM NO ₃ at 90m	EZ O ₂ anomaly well defined at EC	4 0.7/0.5/0.6	Classic enhancement of Fv/Fm in center of transect. Both elevated numbers (highest recorded in this cruise 0.589) and elevation in the water column. The best transect we have seen! Some enhancement in surface waters may be due to day/night sampling. Phytoplankton community dominated by <3µ size class.	(4) Generally low biomass except 50-100m animals .15-1mm.	Tricho and colonial radiolarians
A 5	16-degree mode-water eddy	2 1.0 µM NO ₃ at 90m		3 0.9/1.9/.6	High Fv/Fm values following high Chl. Also high surface values above 20m, possibly due to sampling during the day. Phytoplankton at Chl max in central (24) and eastern edge (30) stations dominated by >5µ size class.	(1) 2x higher biomass than A4 in all depths and size classes except 600- 700m. Very high migrator biomass, shrimp, chaetognaths, euphausiids. High diversity overall	Very thin at surface; mostly small organisms

C5 – almost as strong as BVAL18/19

C3 – classic shape, good contrast in/out, smaller perturbation than C5

A4 – diatom bloom, inertial mixing

A5 – distant origin; similar to A1 from 2004

July 3

VPR survey of A5 completed; VPR/XBT transit to target feature A4 and search for eddy center. Fluorescence from the VPR (Figure 0703.1) indicates high fluorescence inside A5 (center and west of center) and on its eastern periphery. High fluorescence is also evident in the core of A4 as well as in a band near its eastern border (perhaps associated with an apparent convergence in the frontal boundary at 65.25°W).

XBT/ADCP search located eddy center between waypoints #2317 and #2376 to the north (Figure 0703.2). From a physical oceanographic standpoint, either waypoint could be considered eddy center: deeper data (e.g. 600m) favor #2317 to the south, whereas shallower depths (e.g. 50-100m) favor #2376 to the north. VPR data (Figure 0703.3) indicate #2376 lies just to the west of the most intense fluorescence, whereas #2317 is right in the midst of the patch that appears to be running NW-SE. Therefore waypoint #2317 was chosen as eddy center.

Comparing this survey to the prior one on June 24, eddy center appears to have shifted from waypoint #2379 to #2317, or about 63km WSW in 10 days. By fixing EC estimates to the 20km grid of waypoints, we introduce a potential error of 10km in each fix. Therefore the inferred propagation speed is 6 ± 2 km/day, which is consistent with the mean of 5 km/day in this region.

MOCNESS tow at eddy center; CTD survey of A4 begins.

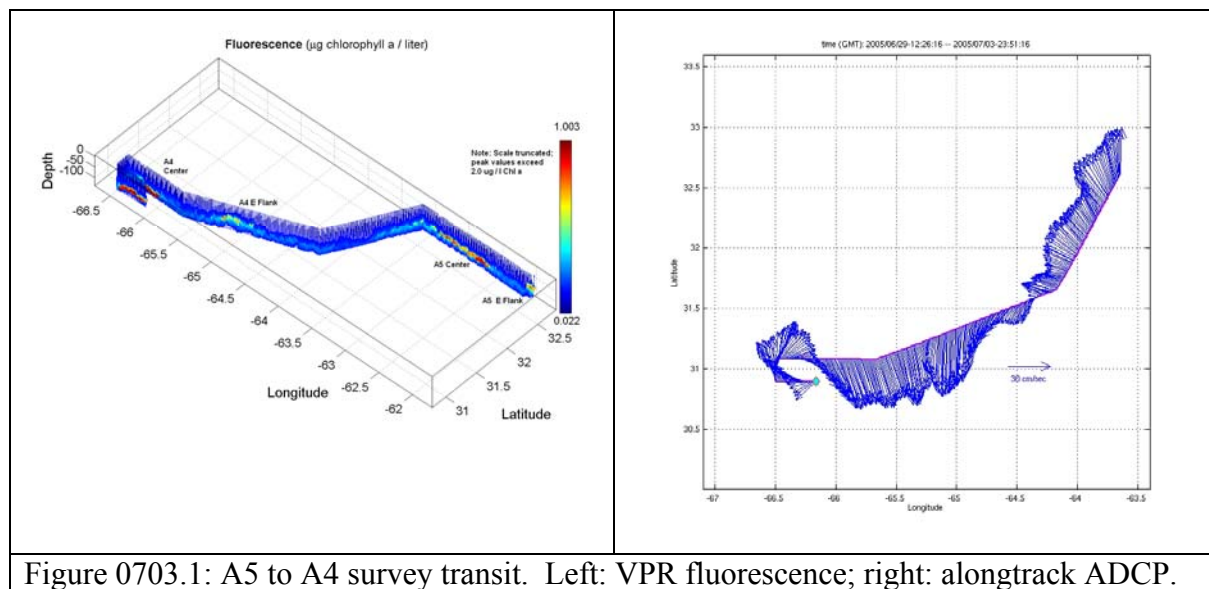


Figure 0703.1: A5 to A4 survey transit. Left: VPR fluorescence; right: alongtrack ADCP.

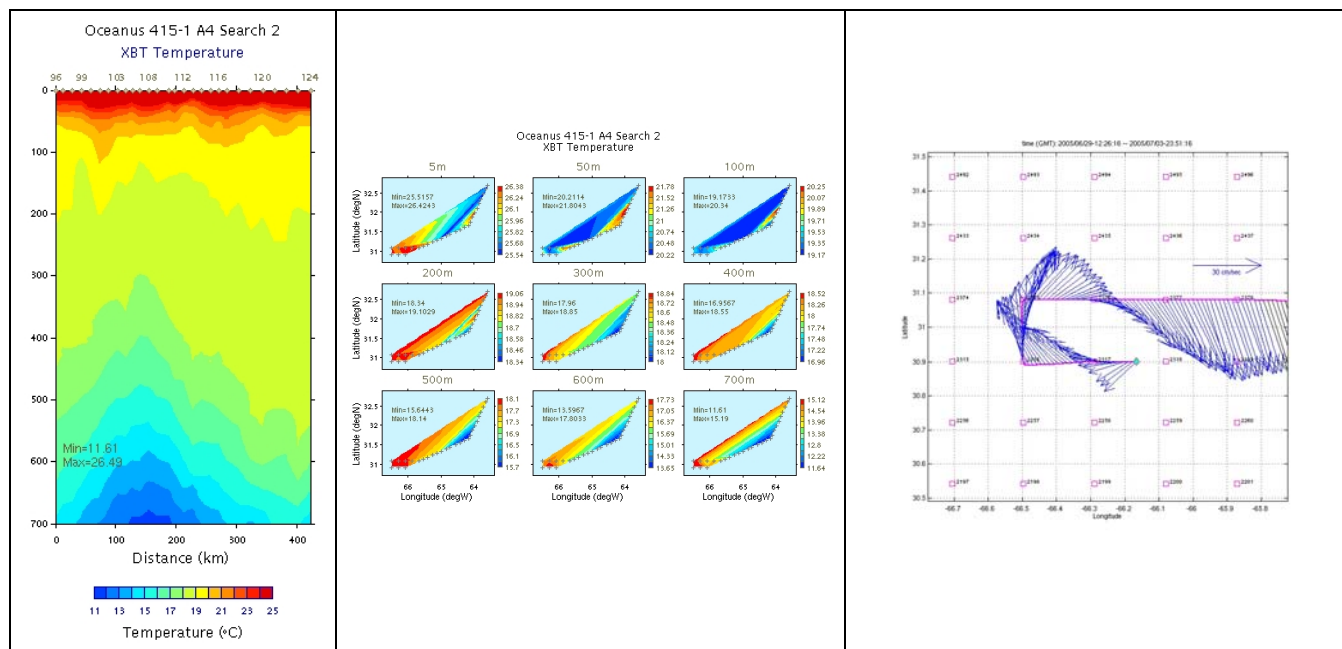


Figure 0703.2: Search for A4 eddy center. Left: XBT temperature section; middle: XBT temperature maps; right: ADCP velocities.

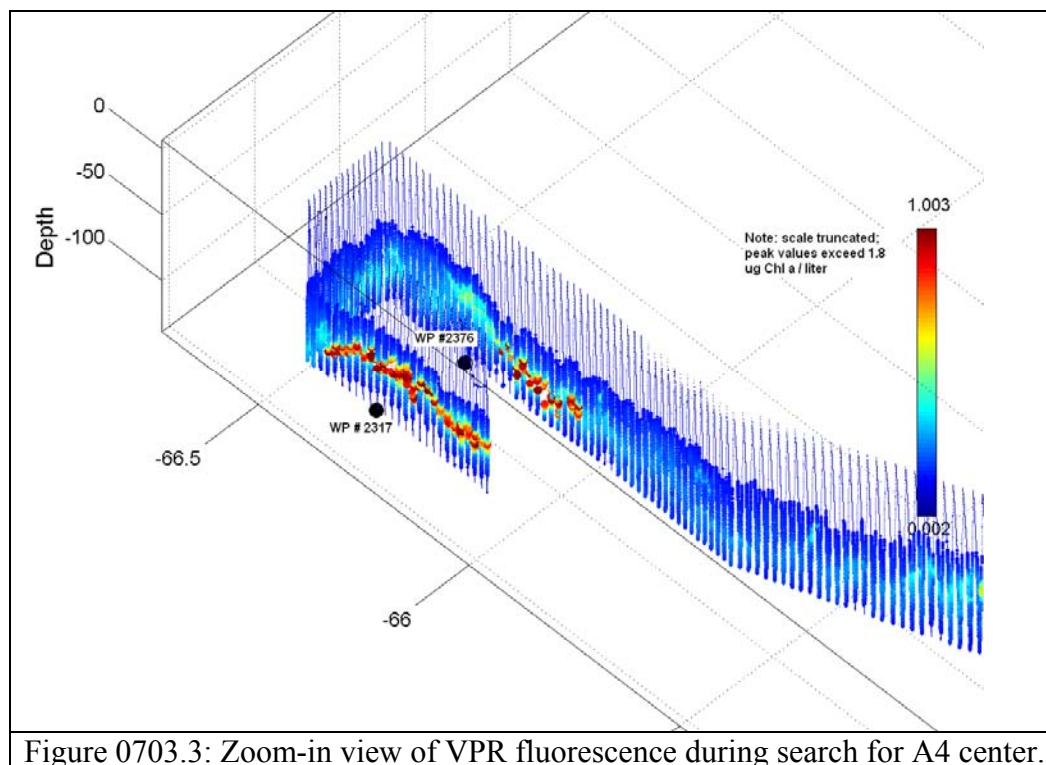


Figure 0703.3: Zoom-in view of VPR fluorescence during search for A4 center.

July 4

CTD survey grid of A4 continues: 3x3 grid at 20km, followed by coarser resolution transects.

Daytime MOCNESS tow at EC; return to EC for another midnight tow.

The high fluorescence patch does not appear to have changed its vertical position appreciably during the time between the two surveys (Figure 0704.1). If anything, there is a little more fluorescence higher in the water column during the second occupation. Nevertheless, the mean depth of the fluorescence maximum is quite deep (100m), with high values as deep as 120m.

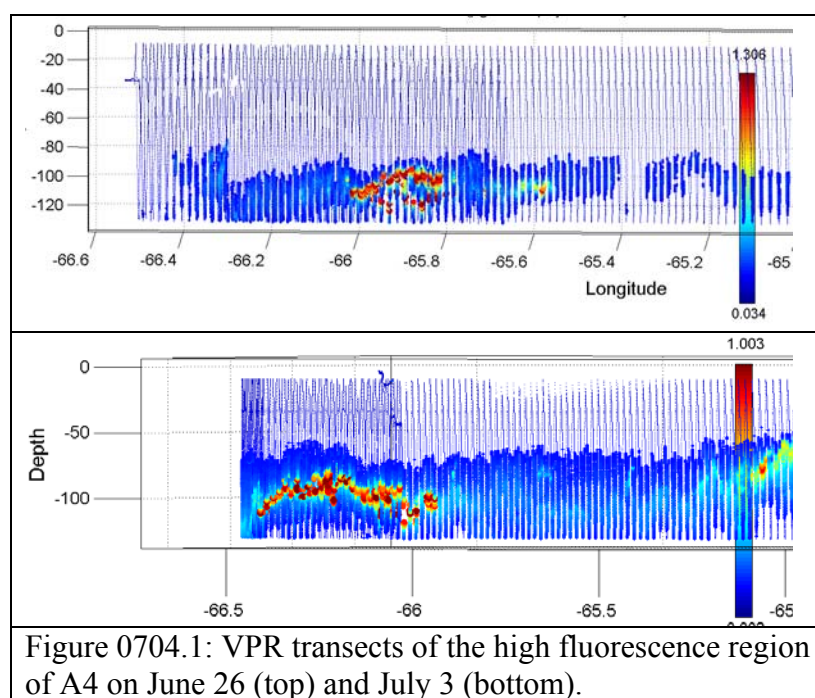


Figure 0704.1: VPR transects of the high fluorescence region of A4 on June 26 (top) and July 3 (bottom).

July 5

CTD survey of A4 continues. Helium/Tritium samples along SE-NW line.

Completion of inner 3x3 grid of 20km resolution CTD stations permits first mapping of A4's inner core (Figure 0705.1). Temperature maps indicate vertical structure characteristic of a mode-water eddy, with warm anomalies at depth (e.g. 600m) and cold anomalies near surface (e.g. 50m). Maps of fluorescence on level surfaces (upper right) show little organized structure, owing to high-frequency vertical displacements of the subsurface chlorophyll maximum (lower right) associated with internal wave activity (lower left). Averaging the fluorescence data in the 80-120m depth interval yields a more coherent map of the field (Figure 0705.2). The band of highest average fluorescence generally runs SW to NE, but its full extent is not yet delimited by

the 3x3 inner grid. The larger scale transects currently underway will quantify the larger scale structure of the bloom.

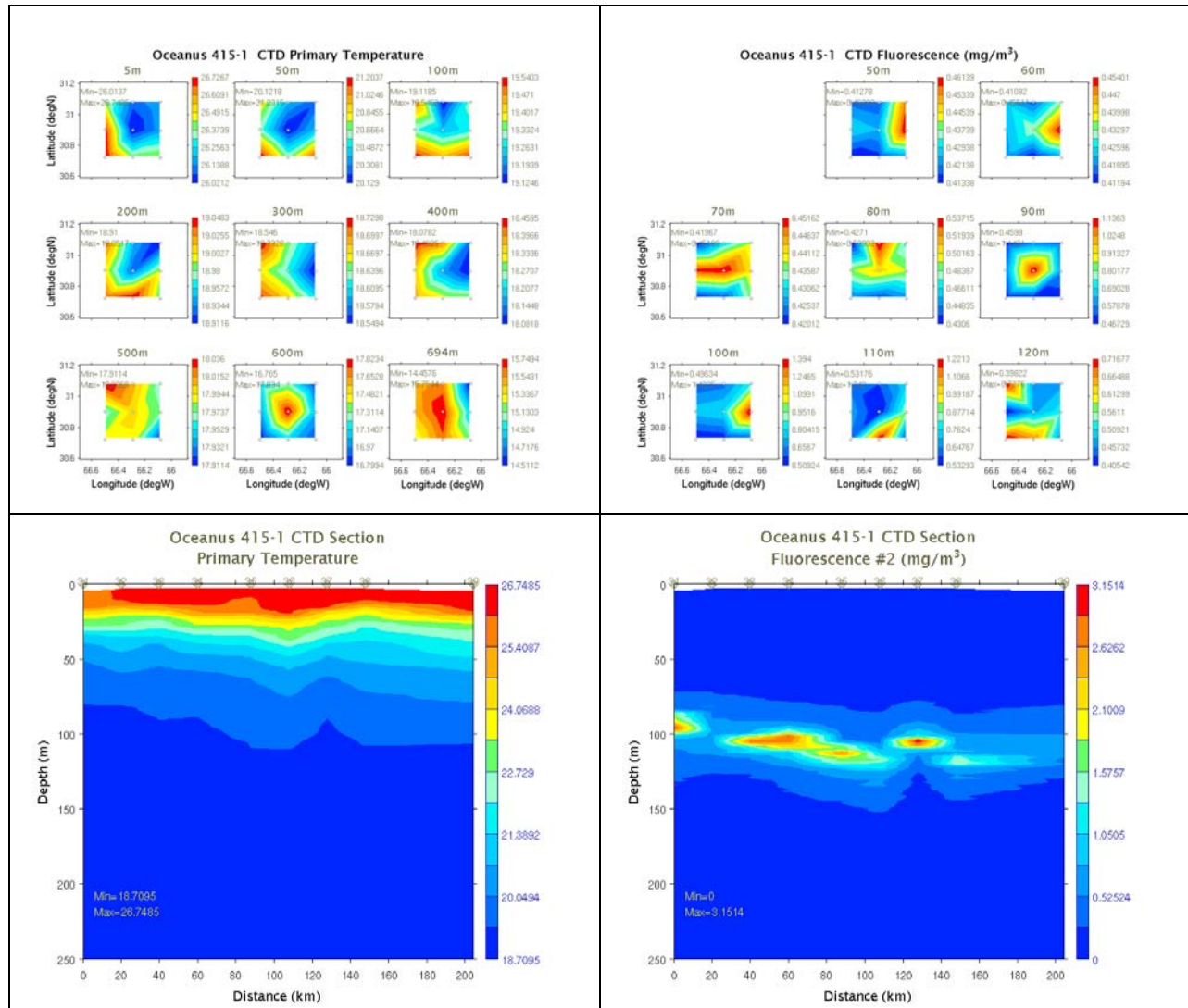


Figure 0705.1: Results of first 3x3 grid of stations at A4 eddy core. Upper panels: maps of temperature and fluorescence; lower panels: alongtrack sections of temperature and fluorescence.

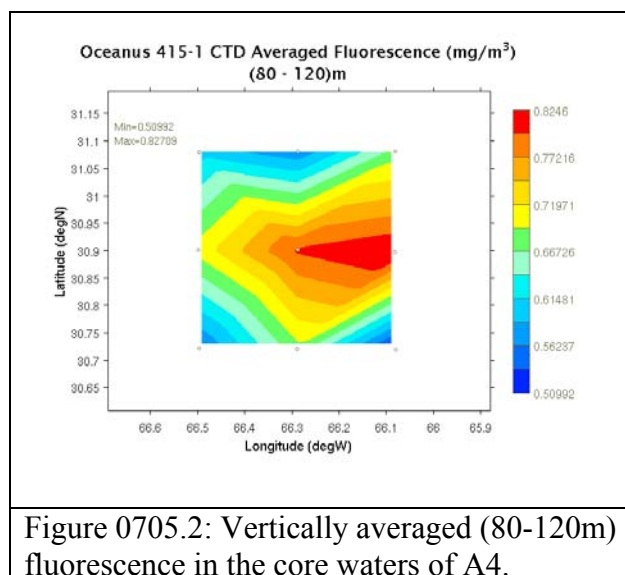


Figure 0705.2: Vertically averaged (80-120m) fluorescence in the core waters of A4.

July 6

CTD survey of A4 continues. Glider deployment at WP # 2494.

ADCP shows velocity fluctuations associated with station stops. No apparent problems with navigation data. ADCP rebooted ca. 1000 hrs at WP #2081; no apparent problems.

MOCNESS tow at WP # 2081; outside A4 due S of center.

July 7

CTD survey of A4 continues.

July 8

CTD survey of A4 continues.

MOCNESS tow at EC # 2317 – daytime.

High resolution nutrient profile to 150.

Supply dropoff from WBII; intercalibration station shortly thereafter.

MOCNESS tow at EC # 2317 – nighttime.

The 150kHz ADCP velocities began to exhibit a dependency on ship speed (Figure 0708.1). The ADCP vectors appear to go in the right direction, but their magnitude is drastically reduced when the ship slowed for station work along track. Troubleshooting various aspects of the diagnostic output did not yield any signs of a problem. In the lack of any thing else to try, the ADCP was

shut down and the computer was rebooted. That appears to have solved the problem. Its cause remains a mystery.

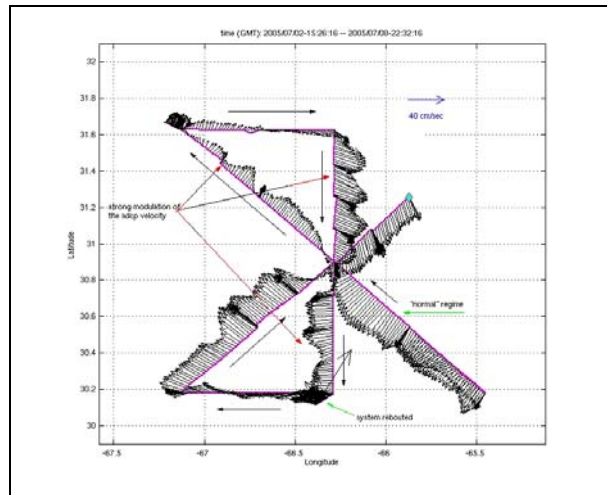


Figure 0708.1: ADCP vectors along A4 survey track.

July 9

CTD survey of A4 completed (Figures 0709.1-5). High fluorescence at eddy center detected on every transect: (1) SE to NW, (2) N to S, (3) SW to NE, and (4) E to W. Peak fluorescence and doming of the seasonal thermocline are tightly confined to EC. The maximum in fluorescence appeared to decrease over time, although that could be due to a shift in EC during the survey.

Nitrate concentration at EC appears stable over time, remaining enhanced over stations slightly off center (Figures 0709.6; data from Qian Li).

MOCNESS tow at NW corner of survey grid (WP #2549) at 1030hrs.

Began ADCP/XBT search for C5 center. Deployed the VPR at 1900 hrs.

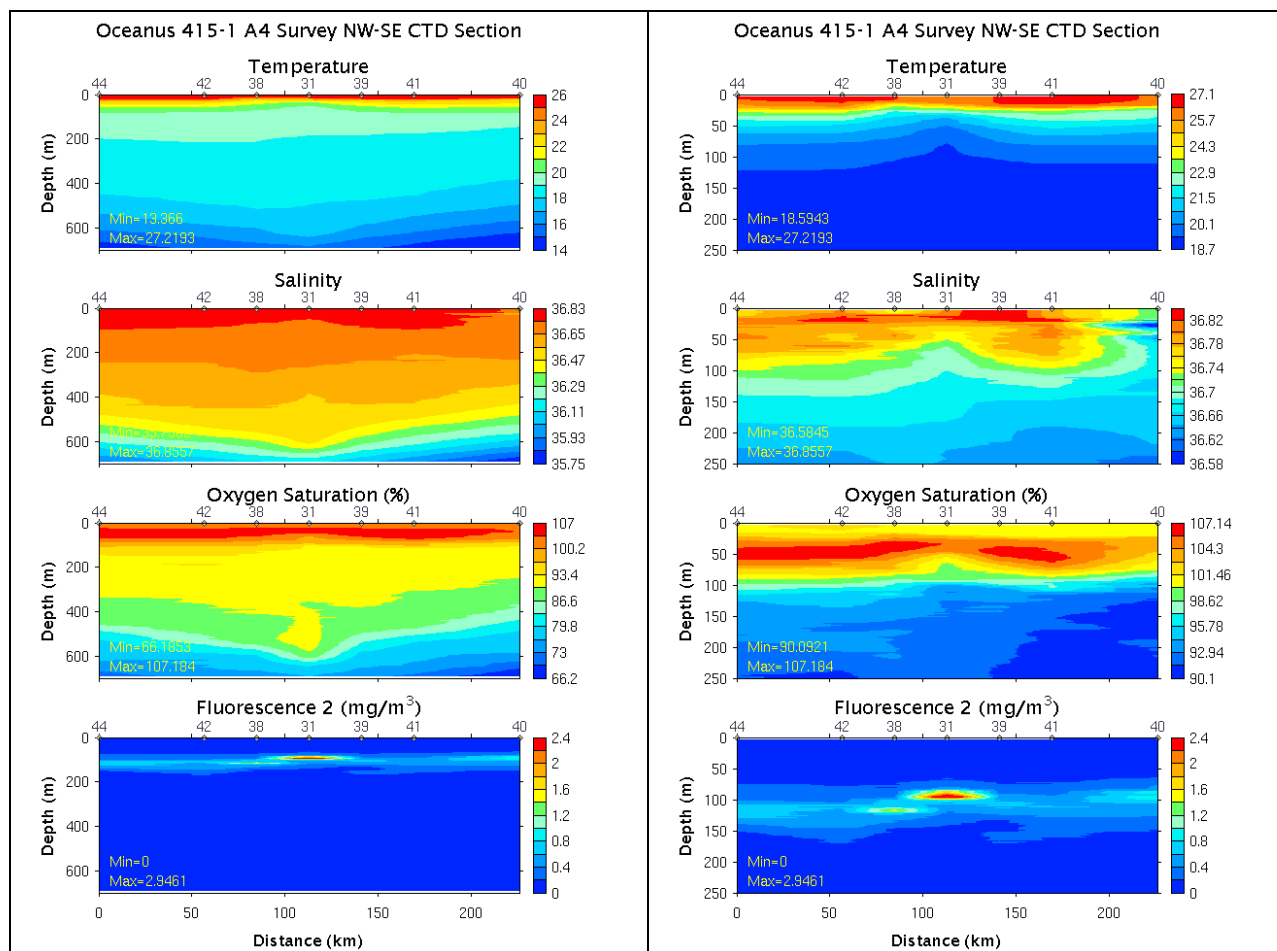
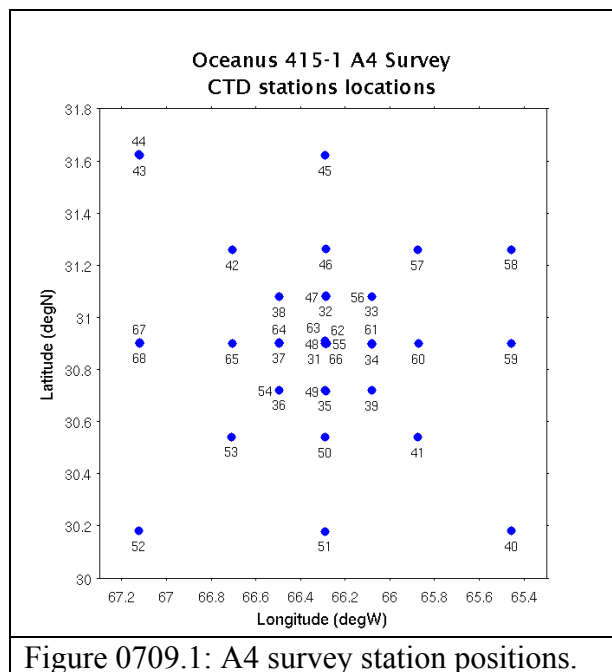


Figure 0709.2: Temperature, salinity, oxygen saturation, and fluorescence (new sensor) across target eddy A4: SE to NW section. Left: 0-700m; Right: 0-250m.

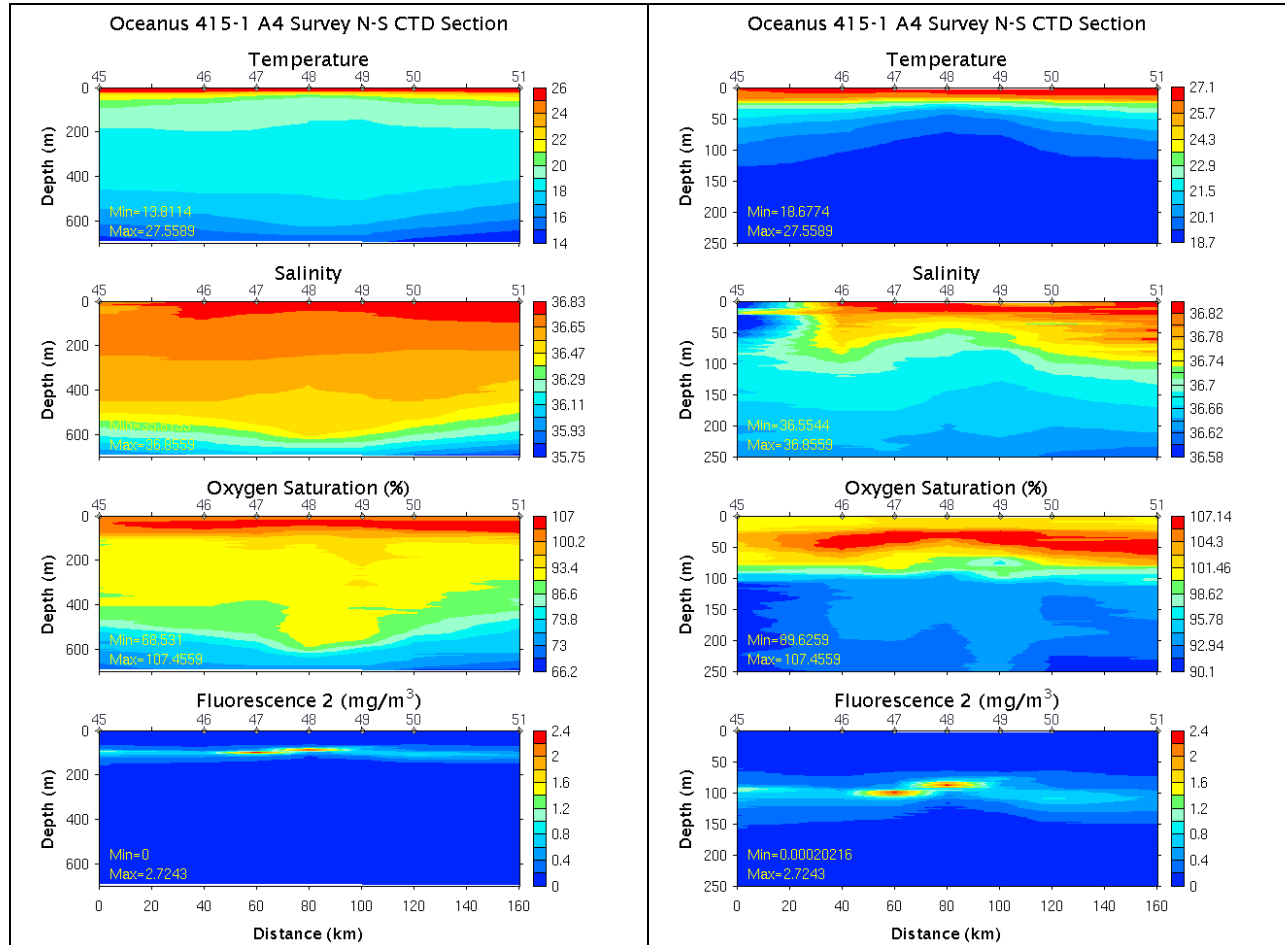
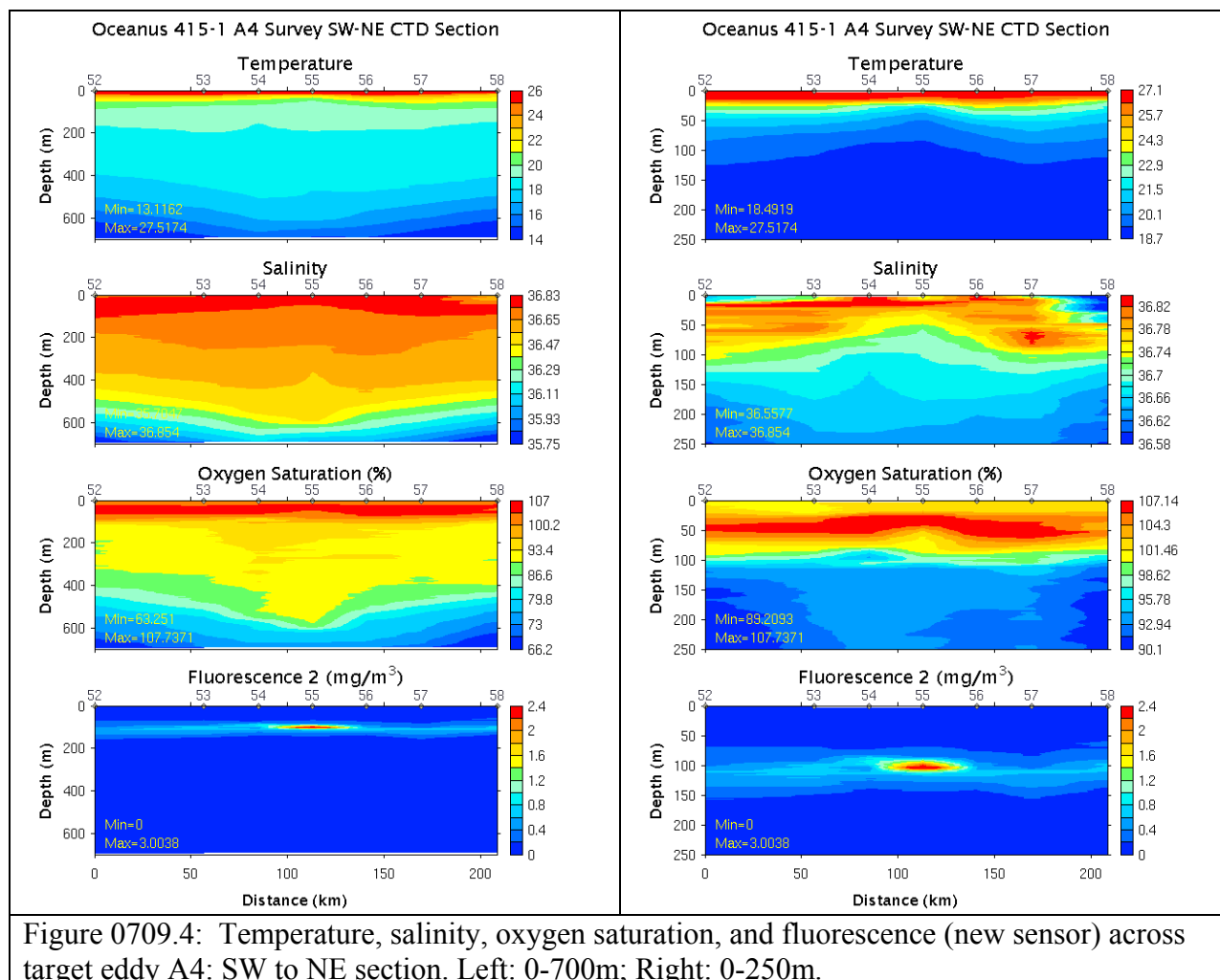


Figure 0709.3: Temperature, salinity, oxygen saturation, and fluorescence (new sensor) across target eddy A4: N to S section. Left: 0-700m; Right: 0-250m.



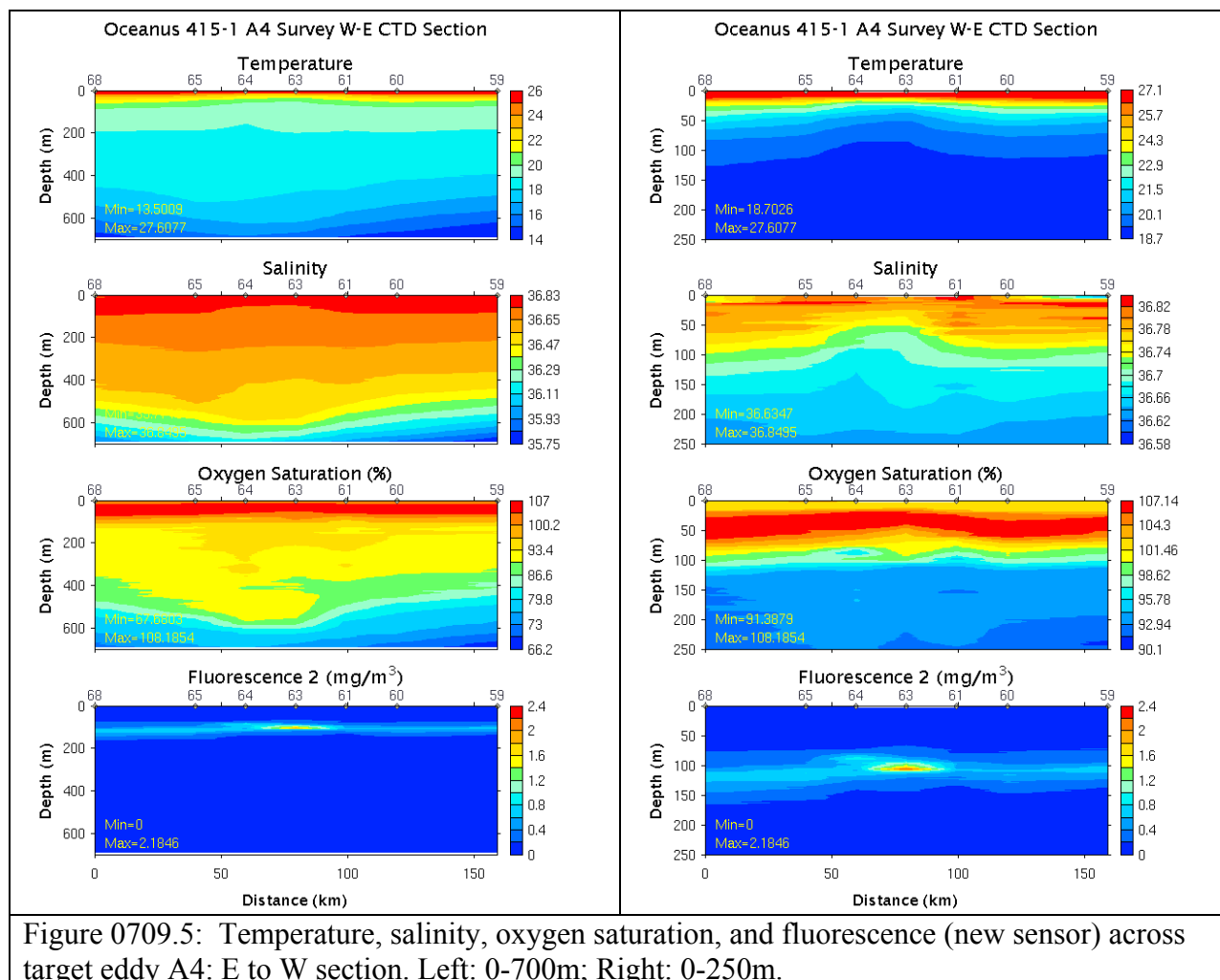


Figure 0709.5: Temperature, salinity, oxygen saturation, and fluorescence (new sensor) across target eddy A4: E to W section. Left: 0-700m; Right: 0-250m.

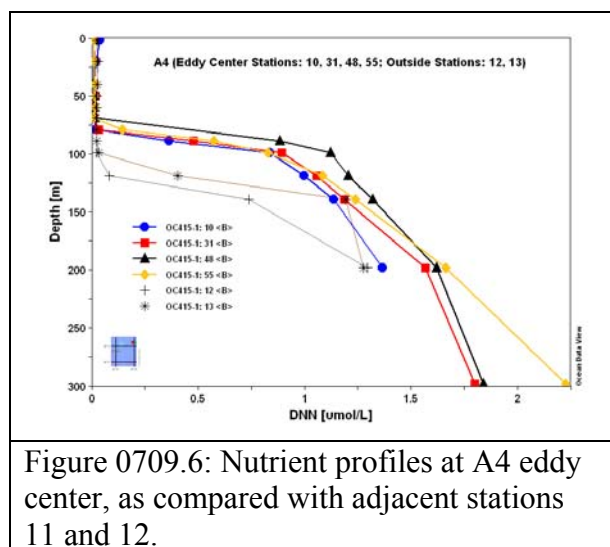


Figure 0709.6: Nutrient profiles at A4 eddy center, as compared with adjacent stations 11 and 12.

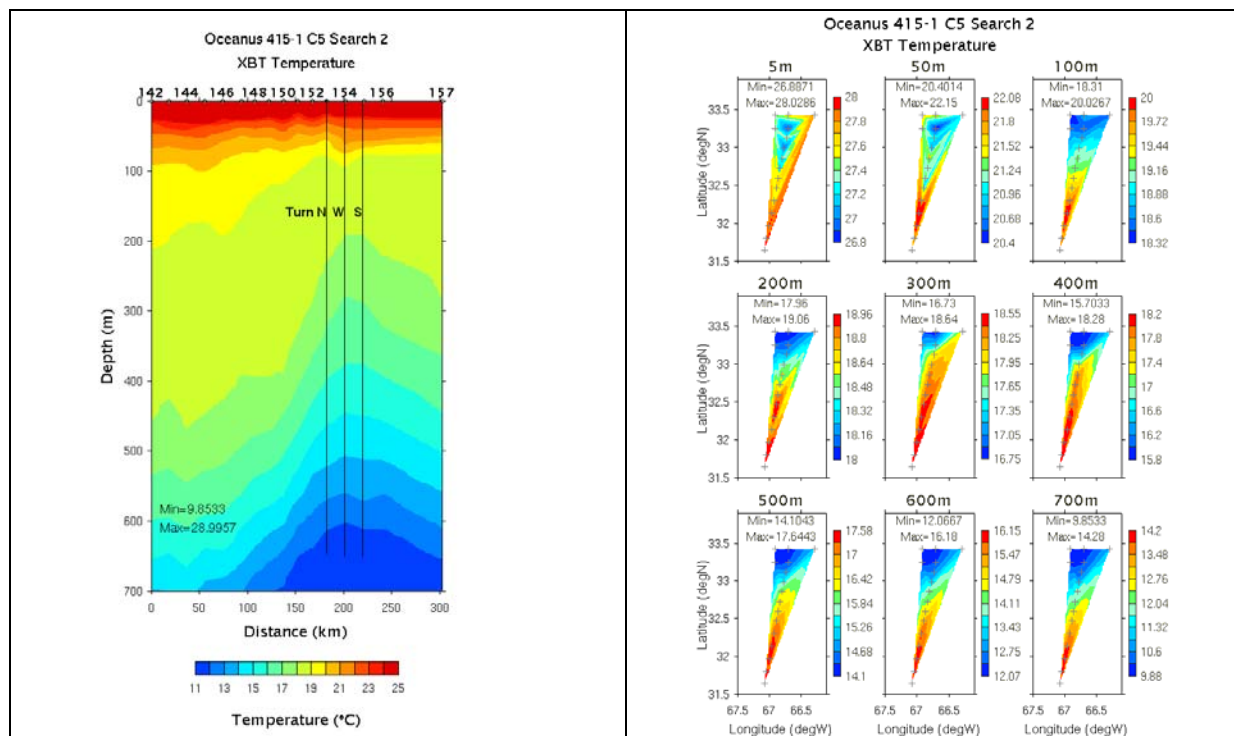
July 10

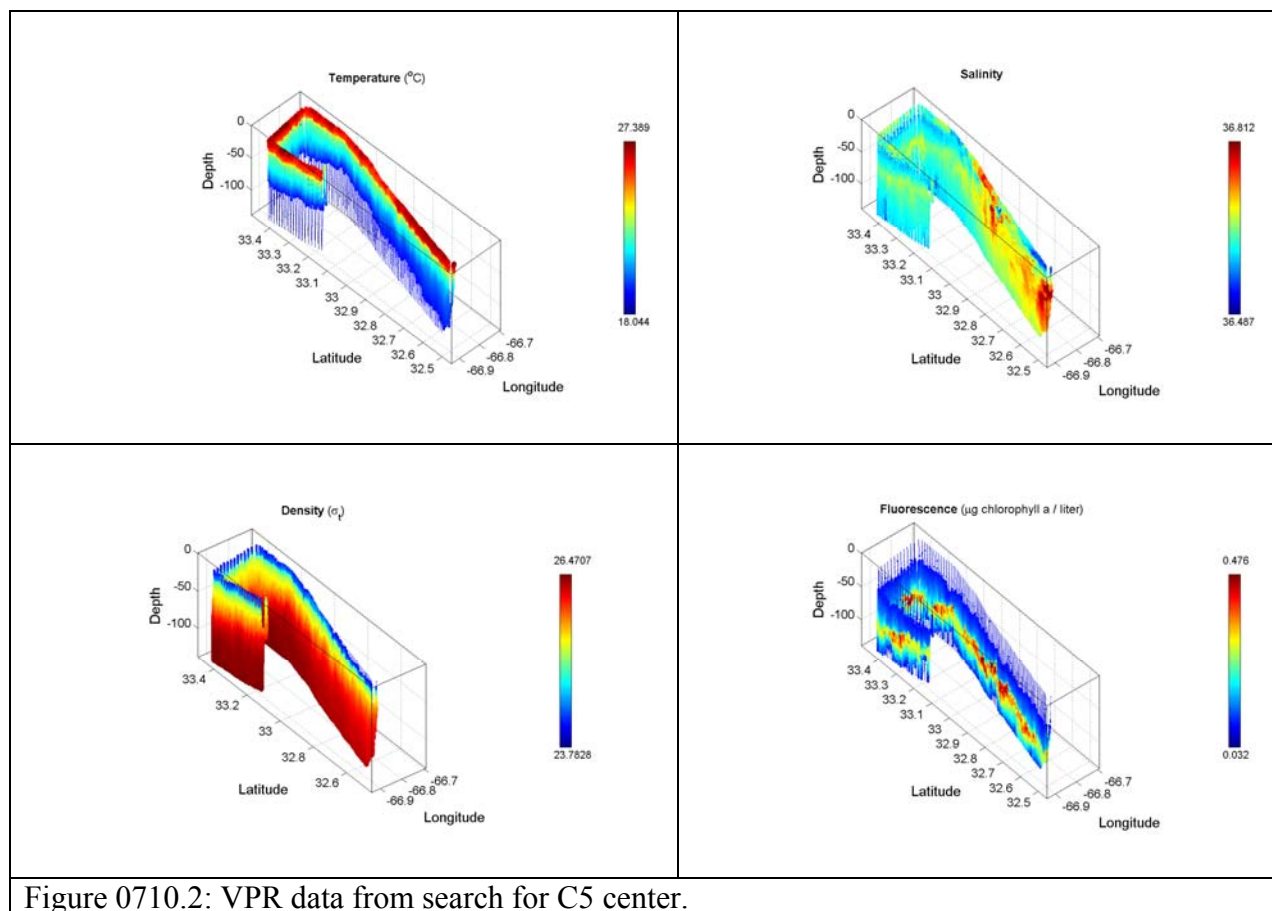
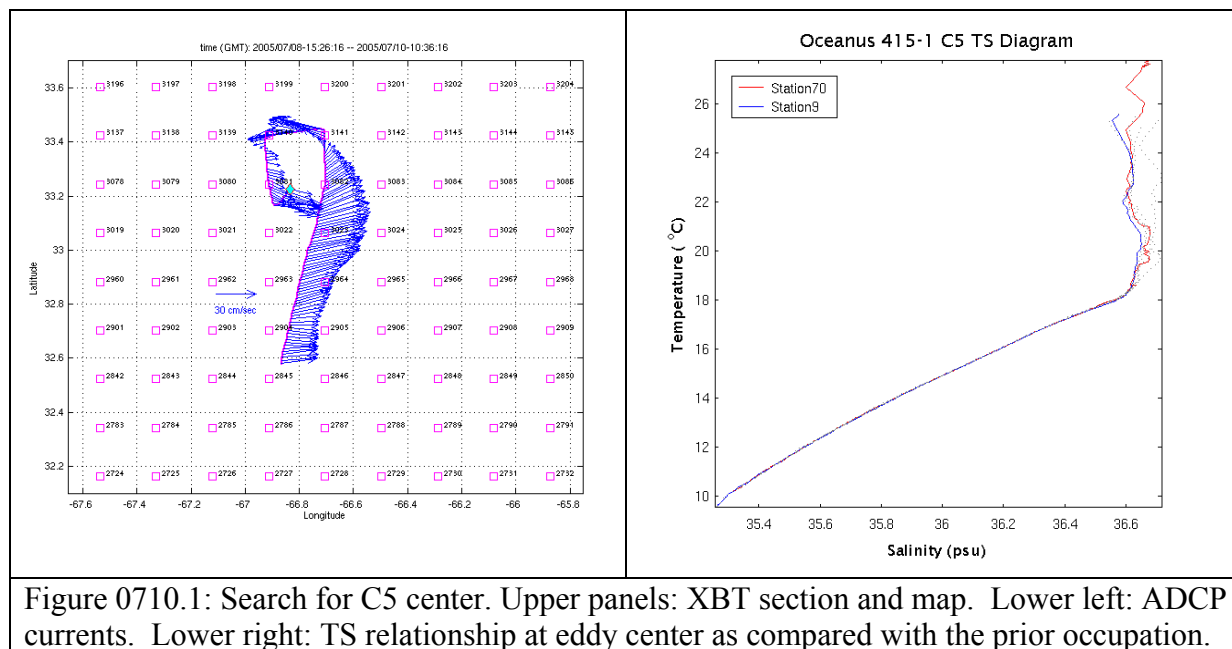
C5 center located at WP# 3141 (Figure 0710.1). Eddy center has moved more than 100km in 17 days since the last occupation, implying a propagation speed of slightly more than 6 km/day. Water mass analysis supports the assertion that this is the same feature we sampled earlier (Figure 0710.1, lower right). Intensity of the feature appears to have diminished, insofar as the magnitude of main thermocline isotherm displacements has lessened from since the last occupation. Data from Qian Li indicates nutrients are still elevated above background levels, but not as much as in the prior occupation.

VPR indicates very low fluorescence overall, with slight enhancement at C5 periphery and in the eddy core (Figure 0710.2).

MOCNESS tow at C5 center.

Incubation cast at C5 center (Bibby).





July 11

CTD section of C5 completed (Figure 0711.1).

Transit to N boundary of A4; VPR deployed.

OS75 ADCP restarted at 1000 hrs to begin comparisons with 150 in order to troubleshoot the problematic behavior: during the failure mode vectors do not make sense, and with fluctuations coinciding with ship starts/stops/turns.

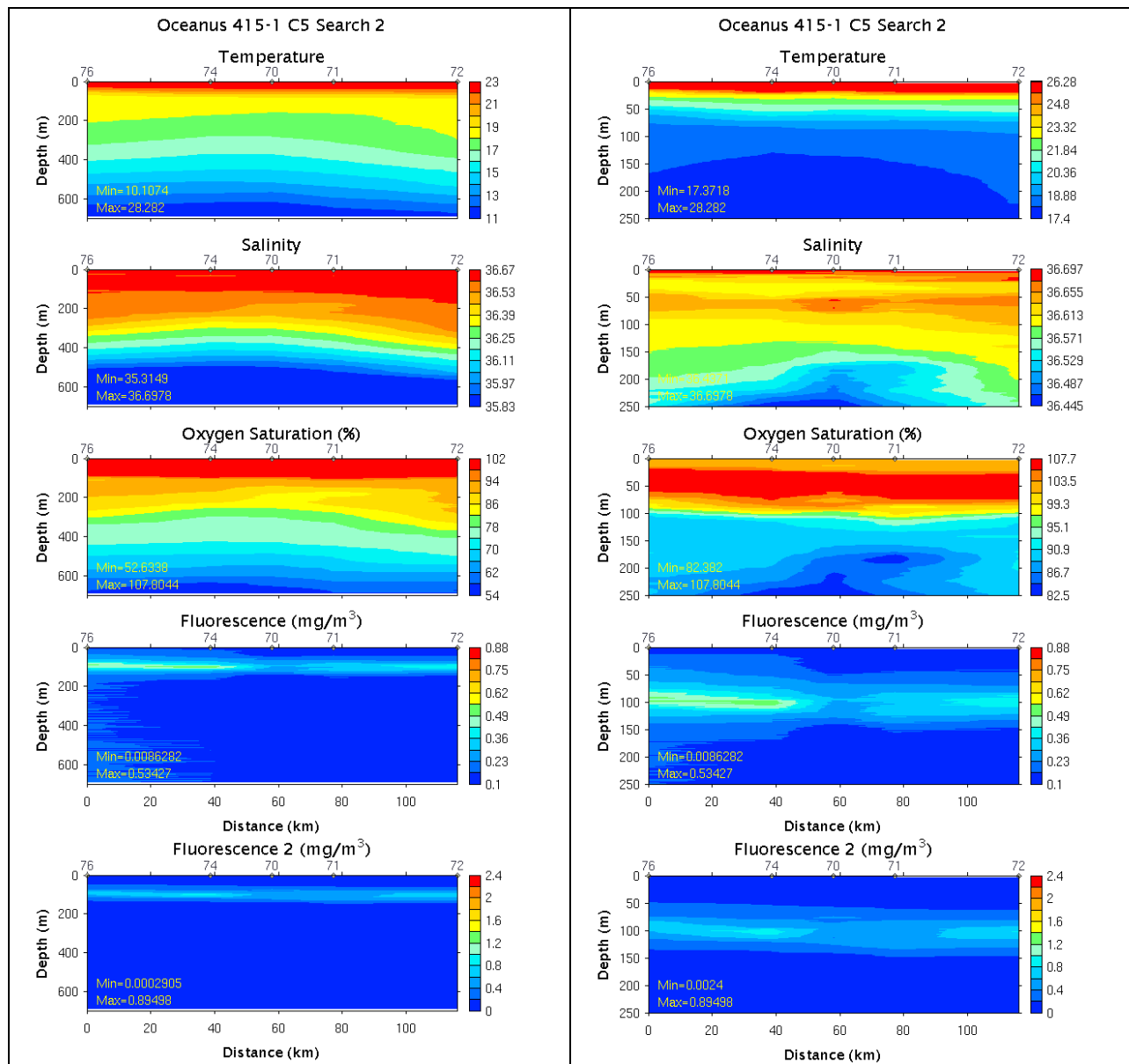


Figure 0711.1: Temperature, salinity, oxygen saturation, and fluorescence across cyclone C5: second occupation. Left: 0-700m; Right: 0-250m. New fluorometer is labeled “fluorometer 2”, and the old fluorometer is included to facilitate comparison with the prior occupation of C5.

July 12

VPR transect from N to S indicates eddy center had shifted away from WP # 2316, the planned position for WBII productivity array deployment at 0430. Trackline available by decision time indicated # 2257 is more in the center of mass of the patch, as opposed to # 2316 just N of the northern edge (Figure 0712.1). This information was passed to the WBII via VHF just prior to decision time. In order to better define the patch in this vicinity, an additional loop to # 2197, # 2256, and back to #2198 was completed before continuing the transect to the south (Figure 0712.2). The patch shows continuity to the east and south, and is clearly not fully delimited by the present loop. Additional high resolution survey work at eddy center is needed.

ADCP and XBT data indicate eddy center now located near the midpoint of 2257, 2198, 2197, and 2256 (Figure 0712.3). Note the apparent temporary dropout of the 150KHz ADCP during the turn at 2256, which is not evident in the OS75 data.

MOCNESS tow at southern periphery of A4 (WP #2021).

VPR redeployed and large-scale survey continues.

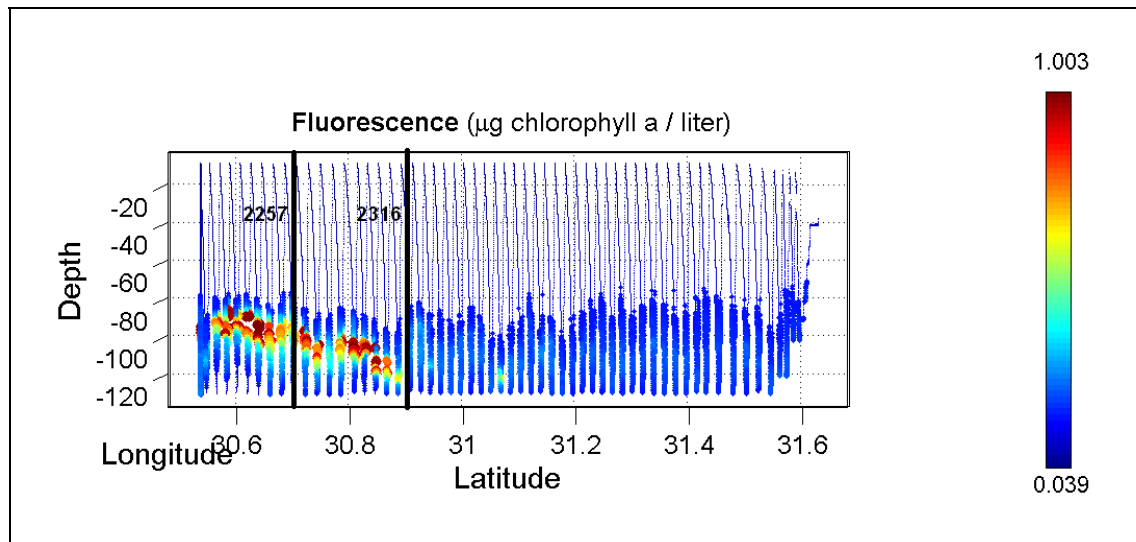
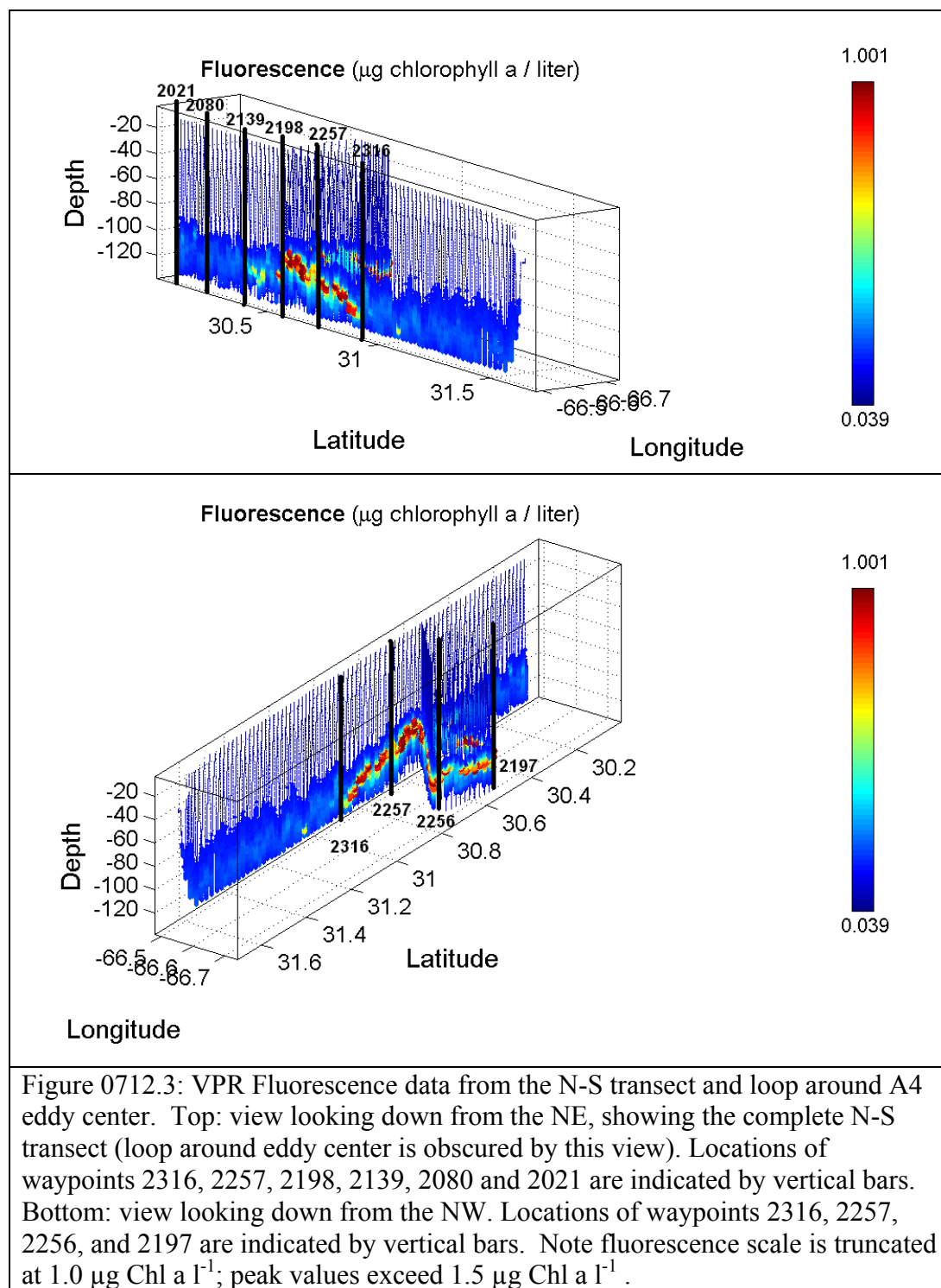
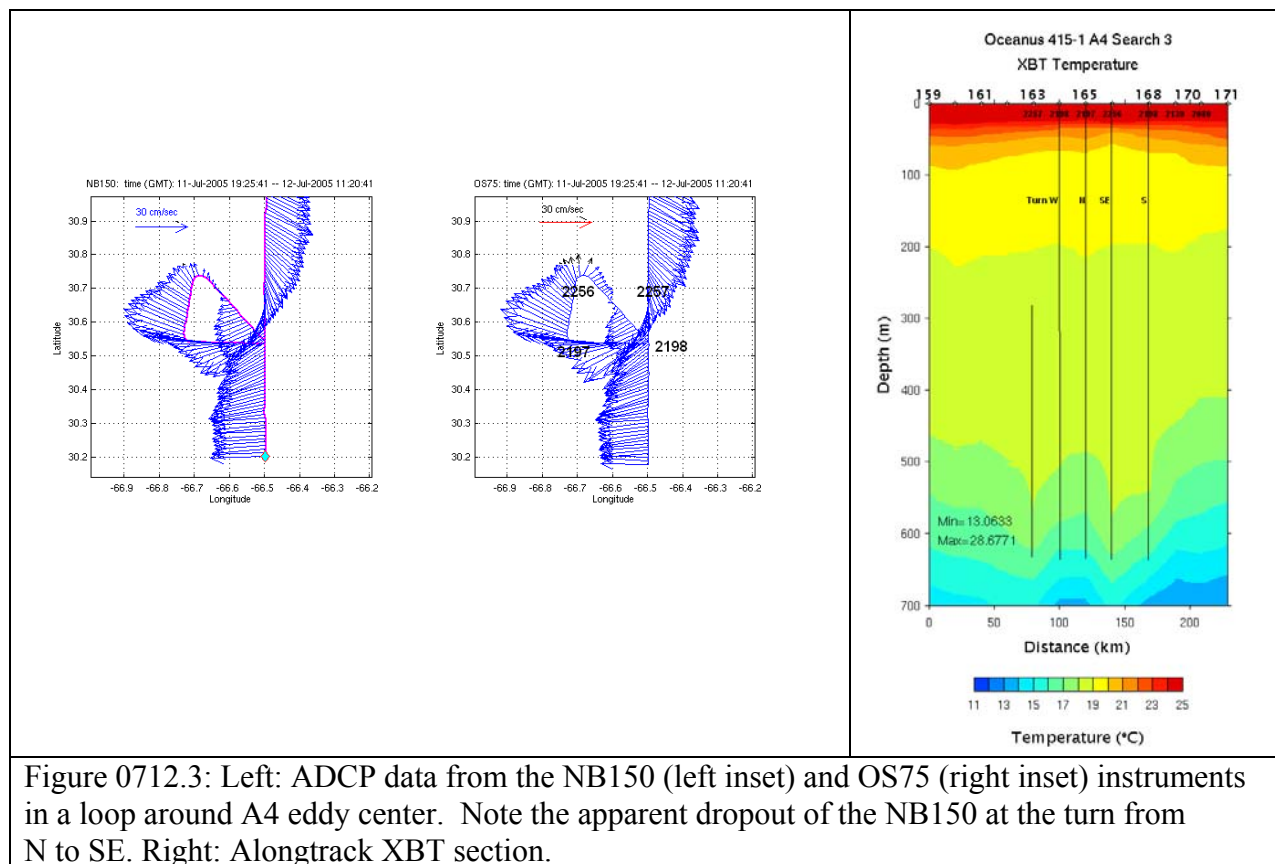
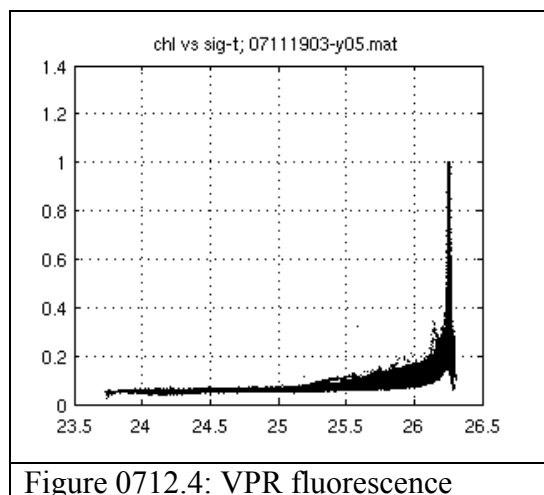


Figure 0712.1: VPR Fluorescence data from the N-S transect available at decision time for siting the WBII productivity array. Locations of waypoints 2316 and 2257 are indicated by vertical bars. Note fluorescence scale is truncated at $1.0 \mu\text{g Chl a l}^{-1}$; peak values exceed $1.5 \mu\text{g Chl a l}^{-1}$.

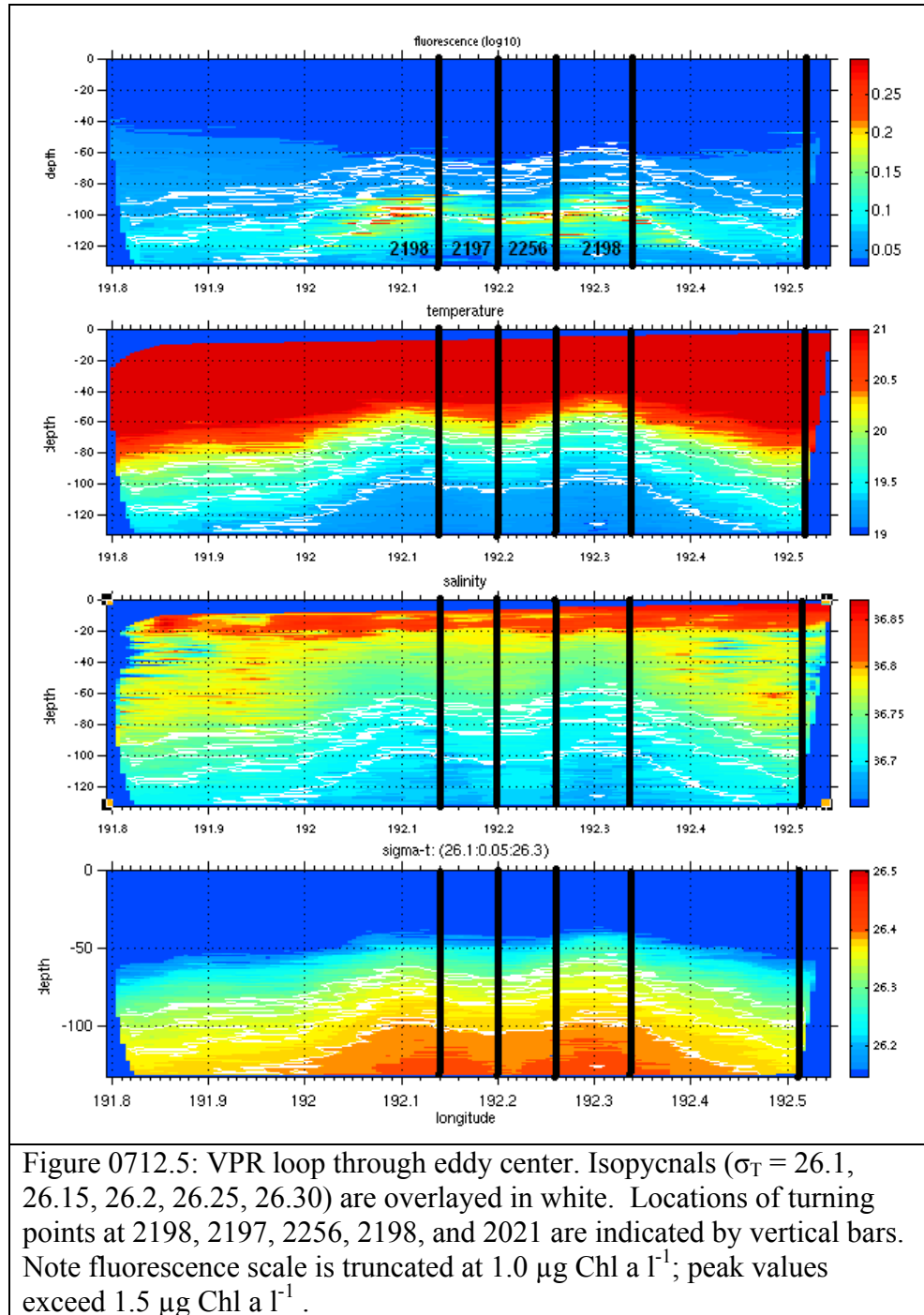




Loop around eddy center (see above) provides reveals the detailed structure of the high fluorescence patch and its relationship to hydrographic structure. Highest fluorescence occurs on the $\sigma_T = 26.25$ isopycnal (Figure 0712.4). At eddy center, $\sigma_T = 26.25$ outcrops into the euphotic zone, rising to just above 100m. This is evident not only in the VPR data (Figure 0712.5), but also in the CTD section across eddy center (Figure 0712.6). Doming of the seasonal thermocline is associated with depression of the main thermocline, with the 18°C isotherm as deep as 575m (Figure 0712.3).



($\mu\text{g Chl a l}^{-1}$) plotted as a function of σ_T during loop through eddy center. Note fluorescence scale is truncated at $1.0 \mu\text{g Chl a l}^{-1}$; peak values exceed $1.5 \mu\text{g Chl a l}^{-1}$.



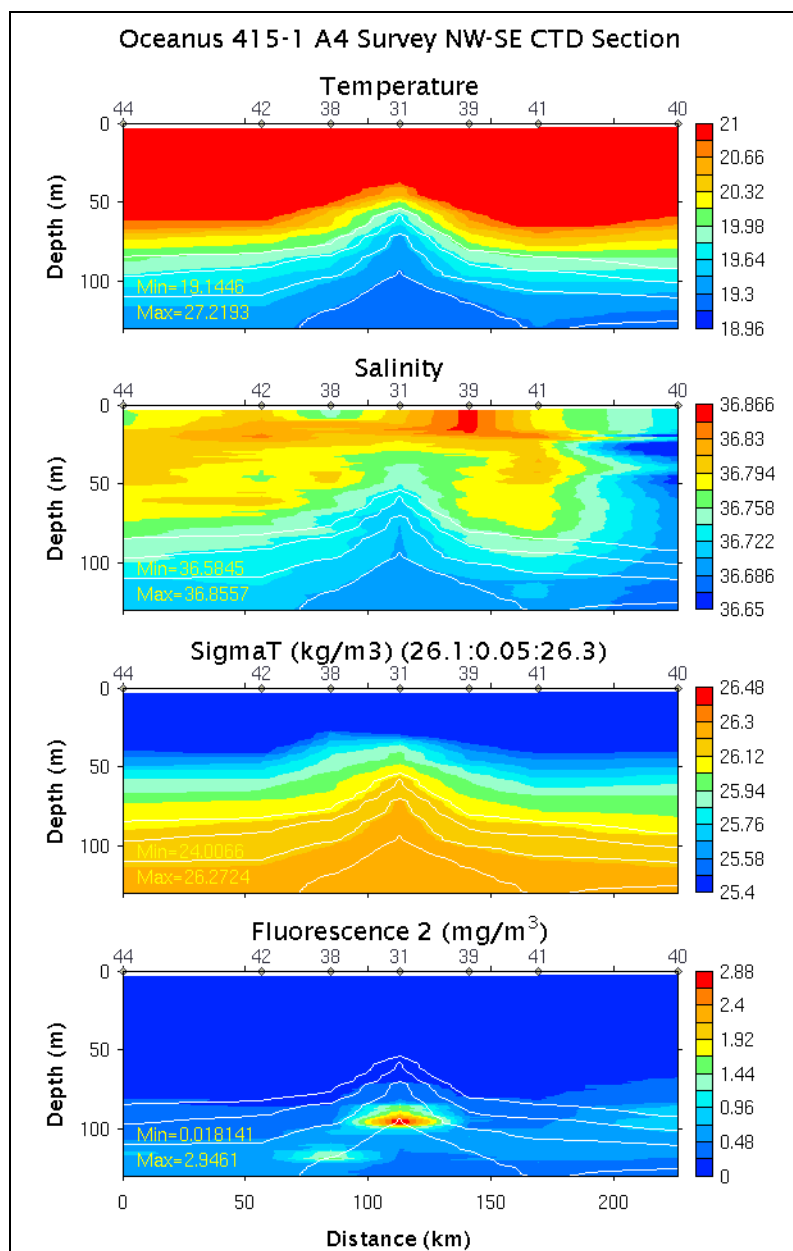
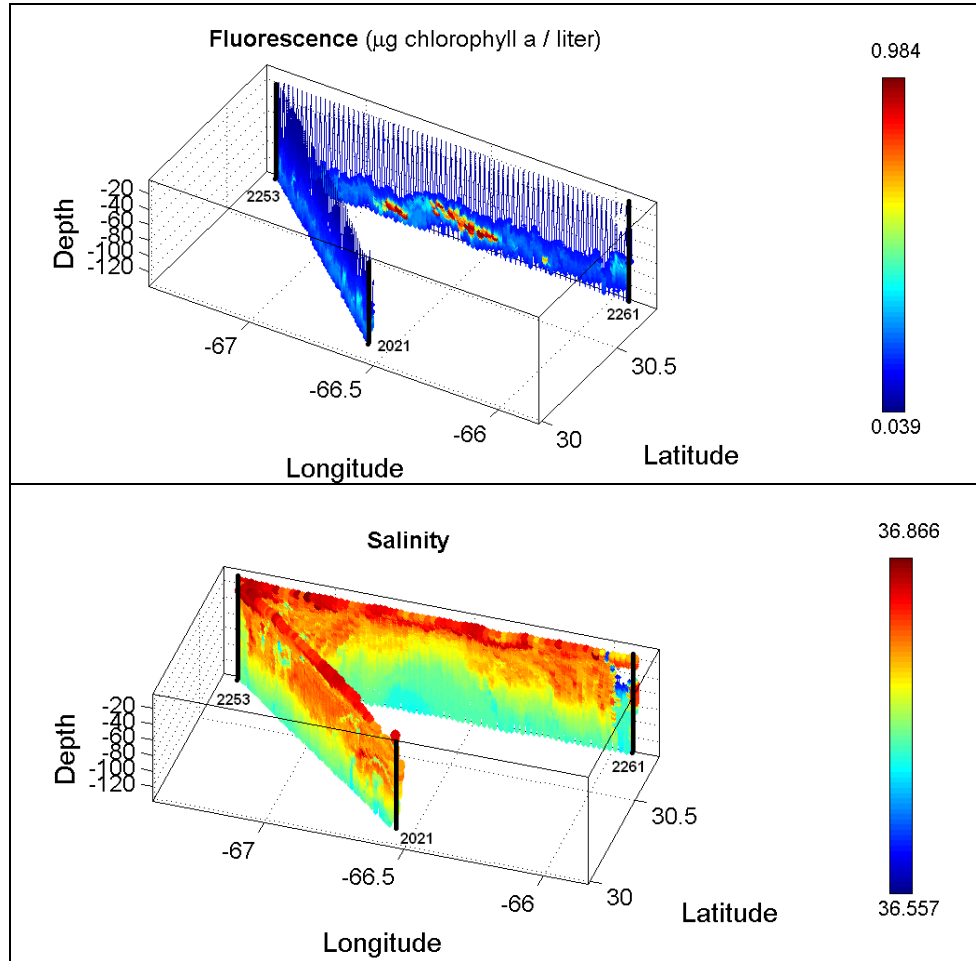
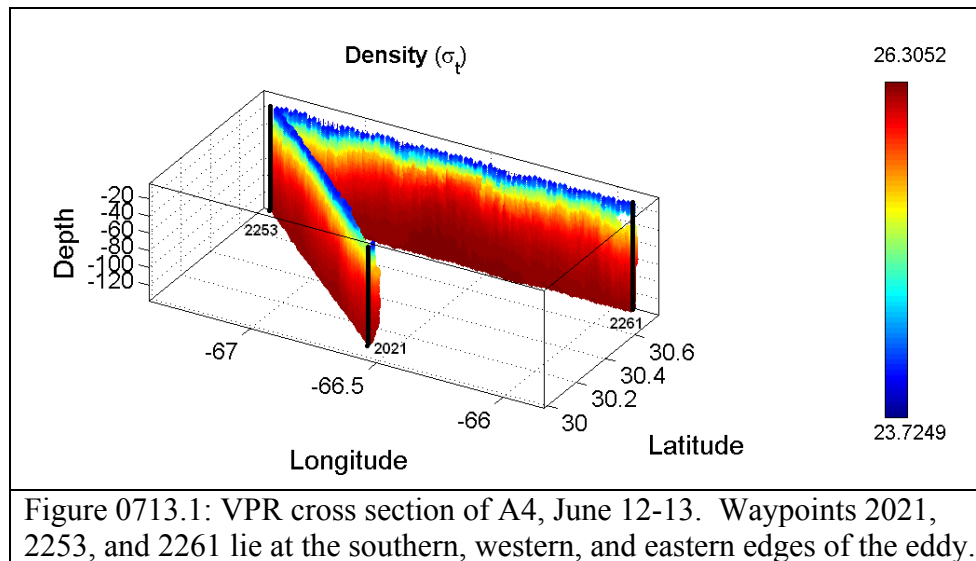


Figure 0712.6: CTD data from NW to SE section across eddy center, using the same color scale as in Figure 0712.5. Isopycnals ($\sigma_T = 26.1, 26.15, 26.2, 26.25, 26.30$) are overlaid in white.

July 13

VPR survey continues. Cross section through eddy center reveals high fluorescence and doming of seasonal pycnocline (Figure 0713.1). Also note salinity structure along eddy periphery.





July 14

VPR survey of A4 completed (Figure 0714.1). Multiple passes through eddy center clearly delineate the extent of the eddy-induced bloom and the high spatial variability within the eddy core (upper panel). The salinity field (lower panel) illustrates doming of the upper ocean pycnocline at eddy center, as well as fine-scale salinity structure at the periphery of the eddy.

CTD cast at 2256 Joint with WBII, companion to productivity array deployment. Waterbury samples collected.

UCSB Spar deployment.

High resolution nutrient/FRRF cast at 2256.

High resolution nutrient/FRRF/pigment cast ca. 20km NW of 2256 where VPR suggests very shallow subsurface chlorophyll max. Profile reveals a jagged peak extending from 80-130m, with measurable fluorescence all the way down to 180m. High resolution profile of nutrients, chl a, HPLC and FRRF down to 200m.

VPR deployed at 2256, towed NE to 2316. Short tow delimits NE extent of the patch.

VPR recovered at 1600, steam to BDA begins.

Incubation cast and Waterbury samples at 2300.

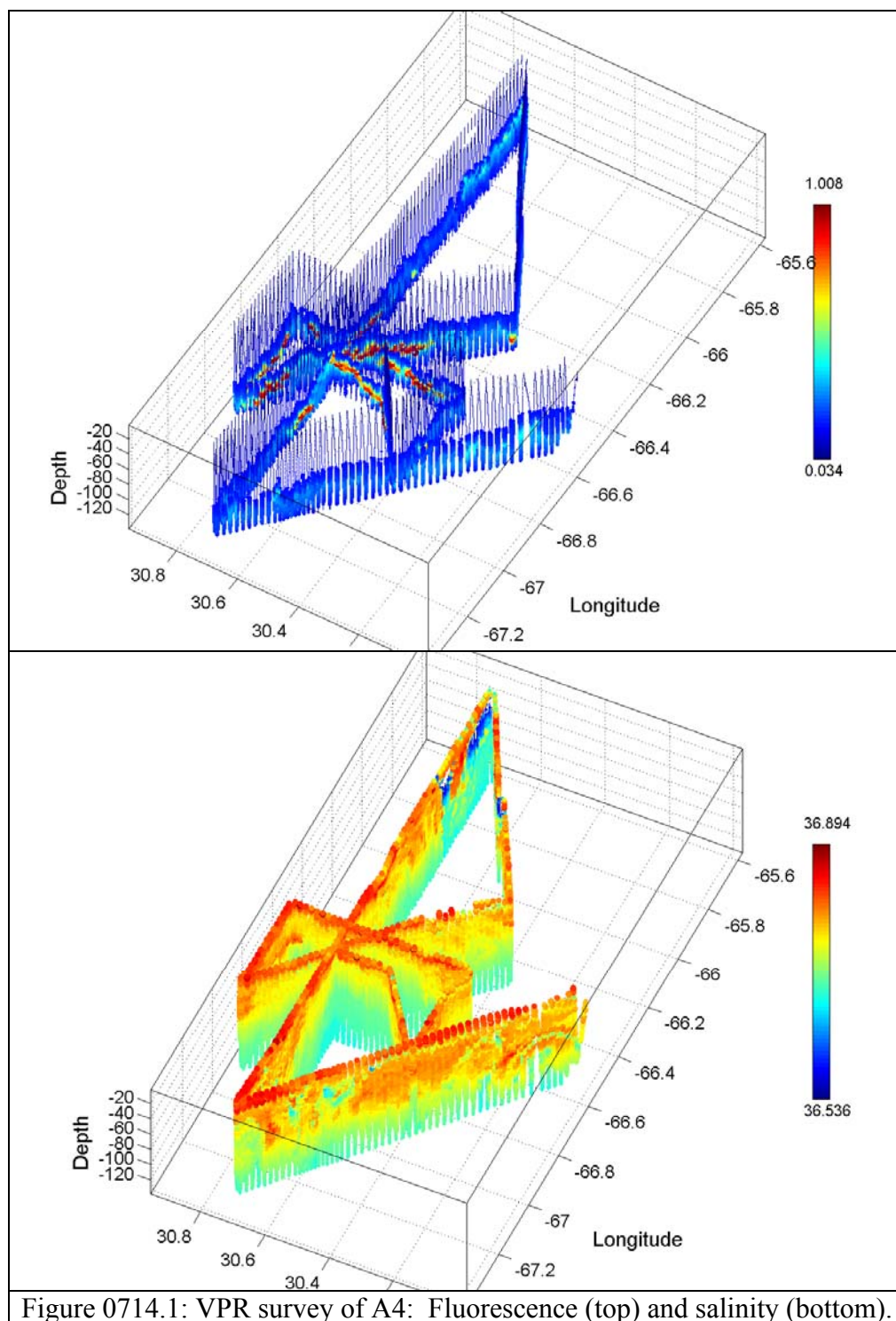


Figure 0714.1: VPR survey of A4: Fluorescence (top) and salinity (bottom).

July 15

Arrival in BDA.

Appendix 1: Selected maps and calibration plots

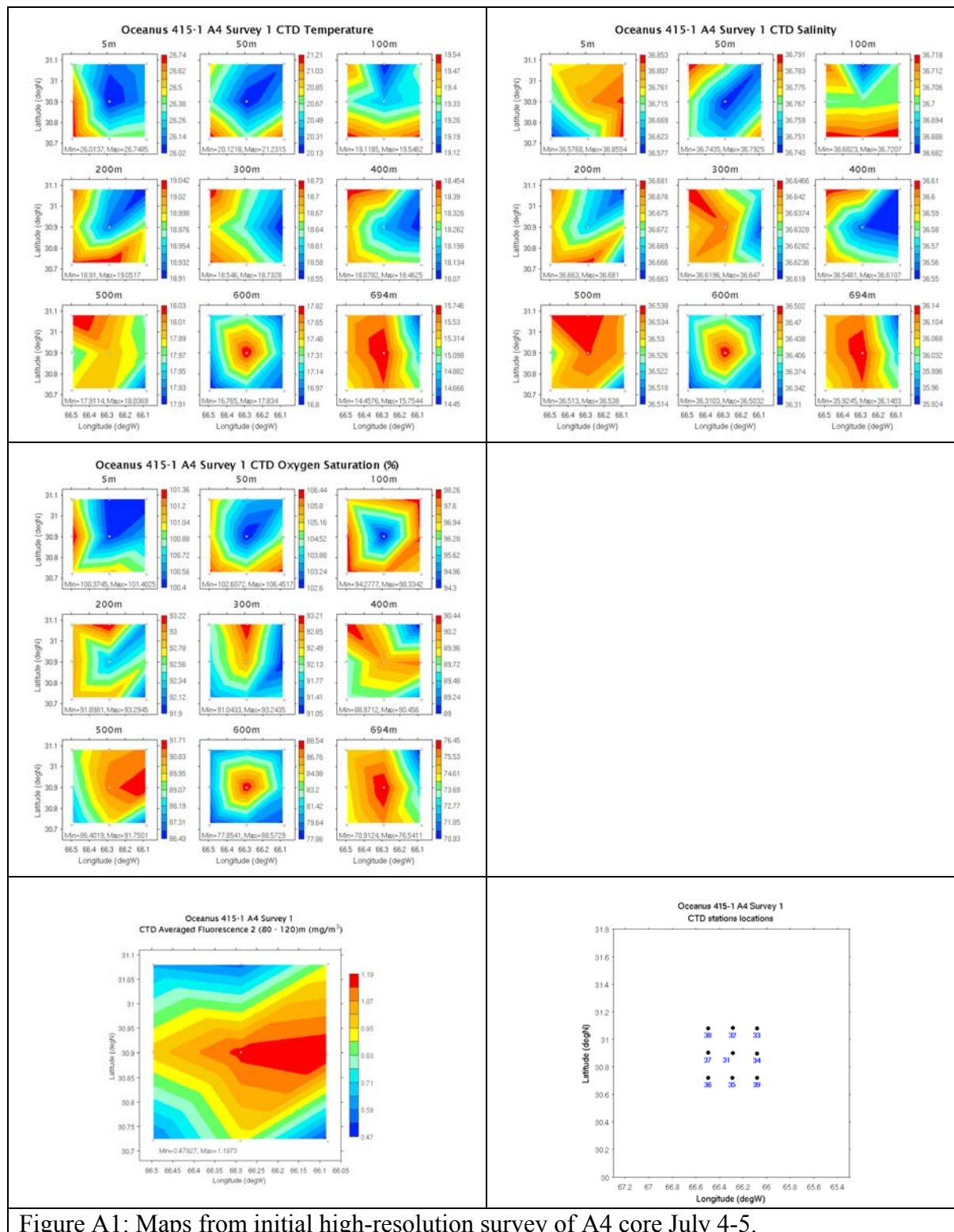


Figure A1: Maps from initial high-resolution survey of A4 core July 4-5.

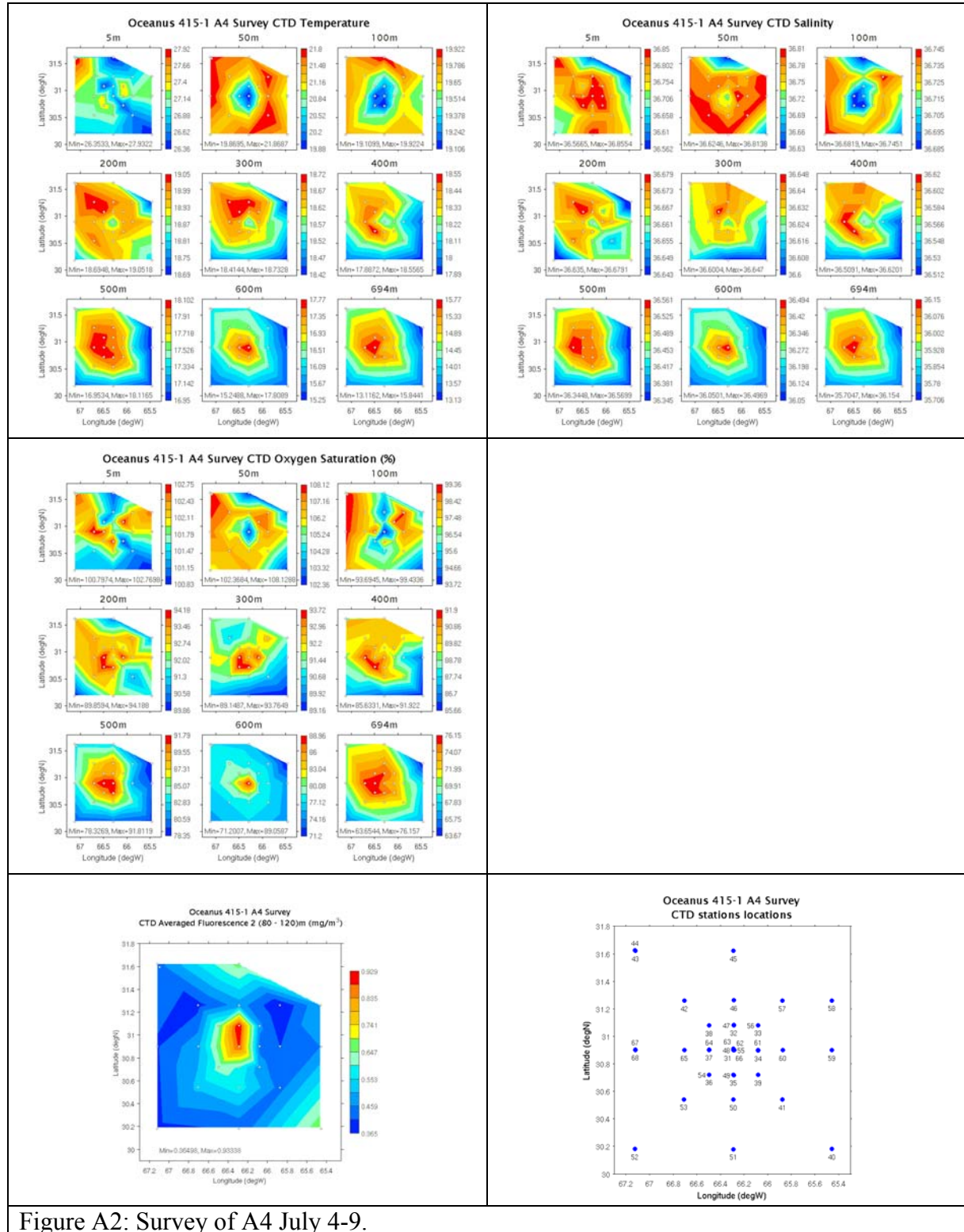
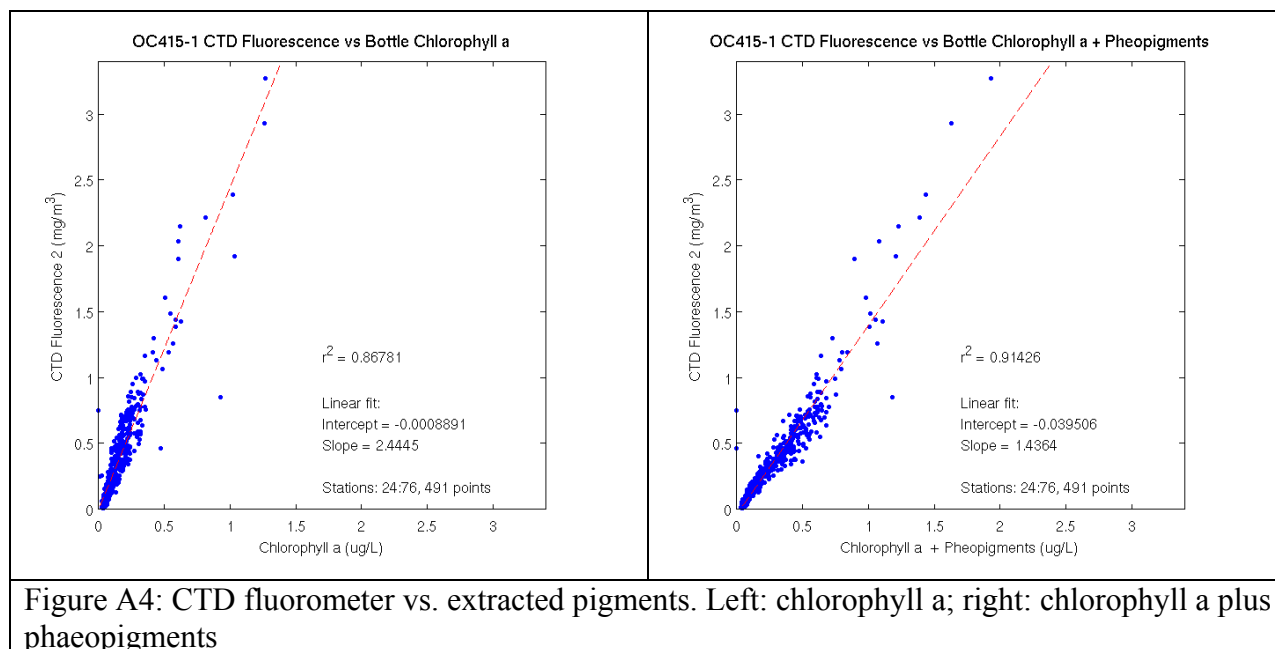
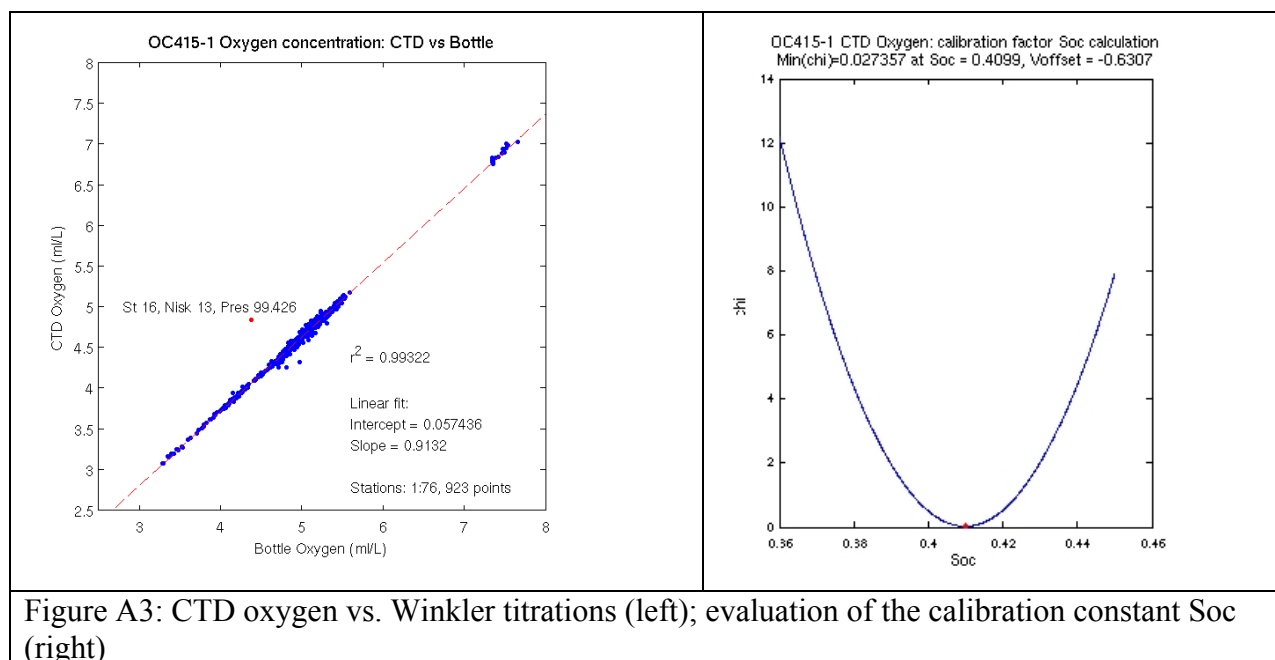


Figure A2: Survey of A4 July 4-9.



Comparison of C5 with the BVAL18/19 Cyclone:

100m Temp	18.1	17.2
700m Temp	9.1	8.5
100m NO3	2.75	4

Appendix 2: VPR deployments

VPR1 – June 24 – C5 cross section (aborted) {ballast problem, flight control software}

VPR2 – June 25 – A4 cross section

File 06260059.y05

VPR3 – June 26 – Starting at A4 chlorophyll patch, heading for C3 {optolink connector to VPR can loose}

File 06262018.y05

VPR4 – June 26-28 – Redeployment following connector servicing.

File 06270248.y05

VPR5 – June 30 – Hydrostation S to A5 (aborted) {optolink connector to flight control can loose}

VPR6 – July 2 – E-W section of A5

File 07020856.y05

VPR7 – July 9-10 – Search for C5 center

File 07092315.y05

VPR8 – July 11 – A4 N-S transect and loop around center

File 07111903.y05

VPR9 – July 12-13 – A4 S periphery to W periphery to E periphery and center survey

File 07121737.y05

VPR10 – July 14 – A4 center (2316) to NE () short tow to delimit NE edge of bloom

File 07141724.y05

Appendix 3: MOCNESS Tows

June 22 – Periphery of C5

June 23 – Center of C5

June 24 – Center of A4

June 28 – Center of C3

June 29 – BATS

July 1 – Center of A5

July 3 – Center of A4 - night

July 4 – Center of A4 – daytime

July 4 – Center of A4 – night

July 5 – Outside of A4 (NW corner) – night

July 6 – Outside of A4 (S of center) – night

July 8 – Center of A4 – day

July 8 – Center of A4 – night

July 9 – Periphery of A4 – day

July 10 – Center of C5 – night

July 12 – Southern periphery of A4 - day

Appendix 4: Incubations

June 23 – Nemmergut and Bibby – Center of C5

Nemmergut:

Ambient O₂ low O₂

Control

PO₄

Fe

PO₄ + Fe high chl

June 25 – Nemmergut – eastern periphery of A4

June 28 – Nemmergut and Bibby – Center of C3

July 2 - Nemmergut and Bibby – Center of A5

July 8 – Bibby – Center of A4

July 9 – Nemmergut – Periphery of A4

July 10 – Bibby – center of C5

Appendix 5: URI underway sampling calibrations (Horne)

Station 9 – June 24

Station 22- June 29

Station 80 – July 14

Appendix 6: Cruise participants

Dennis McGillicuddy, Chief Scientist, Woods Hole Oceanographic Institution

Mr. Valery Kosnyrev, Woods Hole Oceanographic Institution

Ms. Olga Kosnyreva, Woods Hole Oceanographic Institution

Dr. Laurence Anthony Anderson, Woods Hole Oceanographic Institution

Dr. Ilaria Nardello, Woods Hole Oceanographic Institution

Mr. Kevin Cahill, Woods Hole Oceanographic Institution

Mr. Andrew Paul Girard, Woods Hole Oceanographic Institution

Mr. Joshua Eaton, Woods Hole Oceanographic Institution

Mr. Patrick Rowe, Woods Hole Oceanographic Institution

Ms. Megan Jo Roadman, Bermuda Biological Station for Research

Ms. Anne-Christine Pequignet, Bermuda Biological Station for Research

Mr. Qian Li, RSMAS, University of Miami

Mr. Donglai Gong, IMCS Rutgers University

Dr. Thomas Spencer Bibby, IMCS, Rutgers University

Mr. Kevin Duane Wyman, IMCS, Rutgers University

Ms. Diana Reid Nemmergut, IMCS, Rutgers University

Mr. David William Menzies, University of California Santa Barbara

Dr. Sarah Anne Stone, Virginia Institute of Marine Science

Dr. Joseph Sater Cope, Virginia Institute of Marine Science